EFFECTS OF LITHIUM NITRATE ADMIXTURE ON EARLY AGE CONCRETE BEHAVIOR

A Thesis
Presented to
the Academic Faculty

By

Marcus J. Millard

In Partial Fulfillment
of the Requirements for the Degree
Master of Science in Civil and Environmental Engineering

Georgia Institute of Technology

August 2006

EFFECTS OF LITHIUM NITRATE ADMIXTURE ON EARLY AGE

CONCRETE BEHAVIOR

Approved by:

Dr. Kimberly E. Kurtis, Advisor
School of Civil and Environmental Engineering
Georgia Institute of Technology

Dr. Lawrence F. Kahn, Professor
School of Civil and Environmental Engineering
Georgia Institute of Technology

Dr. James S. Lai, Professor Emeritus
School of Civil and Environmental Engineering
Georgia Institute of Technology

Date Approved: July 10, 2006

TABLE OF CONTENTS

LIST OF TABLES

LIST OF FIGURES

SUMMARY

Alkali silica reaction (ASR), a reaction which occurs between reactive siliceous mineral components in the aggregate and the alkaline pore solution in concrete, is responsible for substantial damage to concrete structures in the U. S. and across the world. Lithium admixtures, including lithium nitrate ($LiNO_3$), have been demonstrated to mitigate ASR damage, and are of particular interest for use in concrete airfield pavement construction, where ASR damage has been recently linked to the use of certain de-icing chemicals. Although the effectiveness of lithium admixtures at ASR-mitigation is well-researched, relatively less is known regarding the potential effects, including negative effects, on overall concrete behavior. The goal of this research is to better understand the influence of $LiNO_3$ admixture on early age concrete behavior, and to determine if a maximum dosage rate for its use exists.

Isothermal calorimetry, rheology and bleed water testing, time of setting, chemical shrinkage, autogenous shrinkage, free and restrained concrete shrinkage, and compressive and flexural strength were measured for pastes and concretes prepared with a range of $LiNO_3$ dosages (i.e., 0, 50, 100, 200, and 400% of the recommended dosage). In addition, the interaction of $LiNO_3$ with cement was evaluated by comparing results obtained with six cements of varying alkali and tricalcium aluminate (C_3A) contents. Additionally, one of these cements, was examined alone and with 20% by weight Class F fly ash replacement.

Results indicate that the hydration of the tricalcium silicate and tricalcium aluminate components of cement are accelerated by the use of $LiNO_3$, and that low

alkali cements (typically specified to avoid damage by ASR) may be particularly susceptible to this acceleration. However, inclusion of Class F fly ash at 20% by weight replacement of cement (also common in applications where ASR is a concern) appears to diminish these possibly negative effects of $LiNO_3$ on early age hydration acceleration and heat generation. Dosages higher than the current standard dosage of $LiNO_3$ may have minor effects on fresh concrete workability, causing slight decreases in Bingham yield stress, corresponding to slightly higher slump. Fresh concrete viscosity may also be affected, though more research is necessary to confirm this effect. $LiNO_3$ had no effect on quantity of bleed water in the mixes tested. Generally, $LiNO_3$ had no effect on initial and final setting times, although increasing dosages caused faster set times in the lowest alkali (Na_2O_{eq} = 0.295%) cement examined. In shrinkage testing, higher $LiNO_3$ dosages appeared to cause initial expansion in some sealed paste specimens, but in all cases the highest dosage led to greater autogenous shrinkage after 40 days. In concrete specimens, however, the restraining effect of aggregates diminished shrinkage, and no effect of the $LiNO_3$ was apparent. In no cases, with any dosage of lithium tested, with or without fly ash replacement, did restrained shrinkage specimens show any cracking. Strength testing produced mixed results, with laboratory specimens increasing in 28-day compressive strength, but companion specimens cast in the field and tested by an outside laboratory, exhibited lower 28-day compressive strength, with increasing lithium dosages. Flexural specimens, also cast in the field and tested by an outside laboratory, appeared to show an increase in 28-day flexural strength with increasing lithium dosages. However, because of the conflicting results when

comparing the various strength data, further research is necessary for conclusive evidence of $LiNO_3$ effects on concrete strength.

CHAPTER I

Introduction

Alkali silica reaction (ASR) is a deleterious reaction that occurs in concrete which can significantly shorten the service life of affected structures[1]. Expansive pressure generated during ASR can lead to extensive cracking. In addition to decreasing tensile and flexural capacity and stiffness, this cracking may increase the permeability of the concrete, making it more vulnerable to other forms of degradation. Where cracking has become extensive, spalling of concrete can also occur.

ASR was first identified in 1940 (Stanton, 1940) in bridges and pavements along the California coast. Until recently, ASR damage has been largely associated with pavements, bridges, dams, and other structures with long service lives with ample exposure to moisture. ASR has been identified in many such structures across the United States and the rest of the world (Carse, 2004, Folliard 2005, Pei-xing, 2004). Typically, surface manifestations of ASR damage may take several decades to be apparent.

However, recently ASR-induced damage has been identified at earlier ages, in concrete airfield pavements in commercial airports in Atlanta, St. Louis, Memphis, Denver, Colorado Springs, Salt Lake City, Detroit, as well as at Mountain Home Air Force Base and Andrews Air Force Base, among others. ASR damage has been observed in some of these locations within just a decade of their construction. Spalling is of particular concern with airfield pavements, as "popped-out" aggregate and spalled concrete (i.e., "foreign object debris" or FOD) can cause significant damage to airplanes.

[1] A thorough review of the chemical reactions believed to occur during ASR and the manifestations of damage is provided in Chapter 2 of this thesis.

Additionally, the large costs of replacing airfield pavements after only 15 to 20 years (otherwise useful for 40 to 50 years) have prompted increasing research on preventing damage due to ASR.

Recent research (Rangaraju, 2005) has linked the early onset of ASR damage observed in airfield pavements to alkali-based de-icing chemicals, introduced for use at airfields in the 1990's. Deicing chemicals, such as potassium acetate, potassium formate, sodium acetate, and sodium formate, have been in use since the early 1990's, primarily because they are perceived to be more environmentally friendly than previously used ethylene-glycol based de-icers. These new alkaline de-icing chemicals are applied to airfield pavements before and during storms, and impose on them an alkali load that is likely more severe than may have been anticipated by standard accelerated testing (Rangaraju, 2005). Exacerbating the effect of these additional alkalis, some of these de-icers were found by Rangaraju (2005) to interact with calcium hydroxide in the hardened cement, raising pore solution pH further, and thereby increasing the vulnerability of aggregates to ASR. Rangaraju (2005) concluded that these de-icing chemicals caused expansion and cracking in laboratory specimens, as well as reduction in concrete stiffness as measured by dynamic modulus of elasticity (DME). In some specimens, depending on the test method and aggregate reactivity, expansion occurred with no dependence on cement alkalinity. Previous strategies of mitigating ASR in airfield pavements by limiting the alkali content of cements are largely ineffective considering the effects of these new de-icers.

Figure 1.1. ASR damage at Hartsfield-Jackson Atlanta International Airport

In an effort to avoid or reduce ASR damage in new pavements, lithium-containing additives are being increasingly specified for airfield pavements and other types of construction where de-icing chemicals are used. Lithium compounds were first shown in 1951 to reduce expansion by ASR in mortar bars (McCoy,1951) . In the field, the use of lithium compounds has increased since the early 1990s, with cases of it use in bridge and highway construction in New Mexico, Texas, South Dakota, Pennsylvania, and Delaware (Folliard, 2005).

However, while the use of lithium compounds to reduce expansion by ASR has been well-documented (Folliard, 2005, Johnson, 1997, Lumley, 1997, McCoy, 1951, Stark, 1993), the potential for other variations in concrete behavior has not been previously examined in a comprehensive manner.[2] This uncertainty may increase contractor risk when these additives are specified by owners. For example, during 2004

[2] Further review of the potential effects of lithium additives on concrete behavior is provided in Chapter 2.

reconstruction the Foxtrot and Lima taxiways at Hartsfield-Jackson Atlanta International Airport (H-JAIA), shown in Figure 1.2, concerns were raised regarding the potential effects of lithium compounds on fresh and hardened concrete properties such as workability, shrinkage, and strength gain when the fresh properties of the concrete were not as anticipated. Later it was determined that the observed behavior at H-JAIA was due to an unintentional variation in the mixture design.

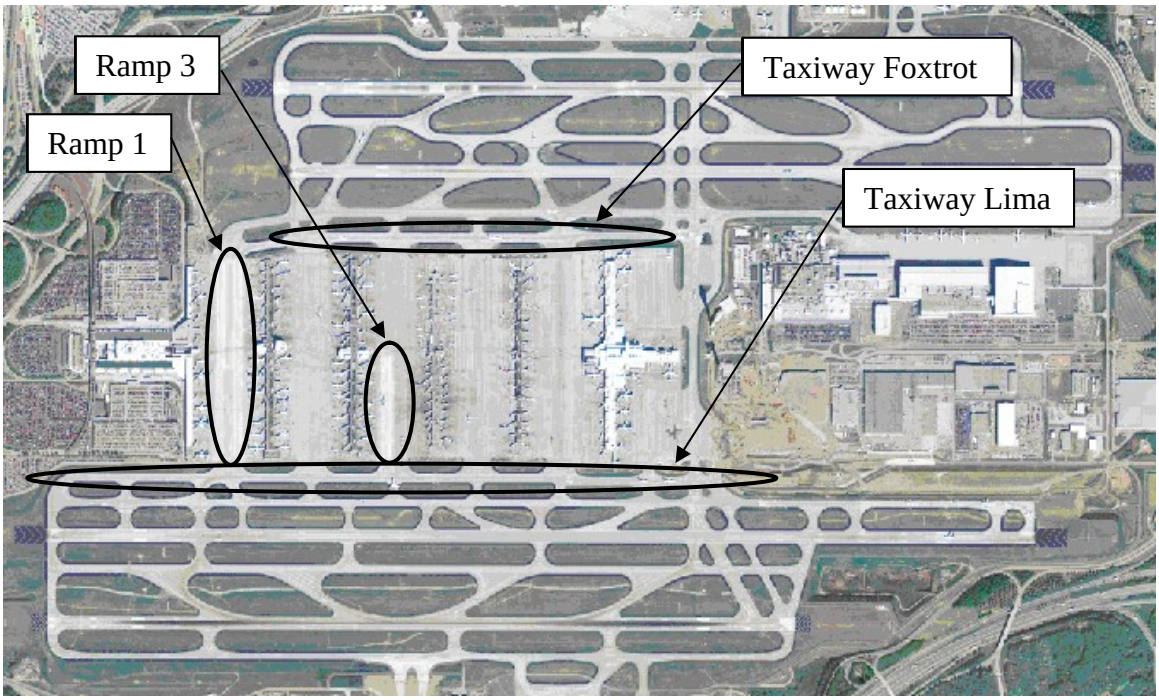

Figure 1.2 Hartsfield-Jackson Atlanta International Airport

Interest in using lithium admixtures at higher than usual dosage rates has increased, in an attempt to provide additional or longer term protection from ASR damage. However, the effects of these larger dosage rates - as with the effects of the recommended dosage rate - on concrete behavior have not been the subject of a prior comprehensive investigation.

The purpose of this research is to holistically examine any potential effects of a lithium admixture on concrete behavior. Lithium nitrate ($LiNO_3$) was selected for this research because it is currently the most commonly used lithium compound for ASR suppression. To identify any upper lithium dosage limit above which negative effects may occur, the behavior of mixtures prepared at several lithium dosages, up to four times the accepted standard effective dosage, are examined. Effects of lithium nitrate on the early age behavior of six cements of differing alkali and tri-calcium aluminate (C_3A) contents are investigated. In addition, one of these cements was tested with 20% by mass Class F fly ash replacement. The behaviors examined in this research included heat of hydration, workability measured by slump and rheometer testing, concrete bleeding, time of setting, chemical shrinkage, autogenous shrinkage, free and restrained concrete shrinkage, and concrete compressive and flexural strength.

Of particular interest in this research is the use of lithium nitrate in airfield pavements. Concurrent with laboratory testing at Georgia Tech, reconstruction of Ramps 1 and 3 at Hartsfield-Jackson Atlanta International Airport, shown in Figure 1.2, has provided an opportunity to observe the behavior of field concrete dosed with lithium nitrate. Results of laboratory testing at Georgia Tech were complemented by compressive and flexural strength data from full scale batches from this reconstruction.

CHAPTER II

Literature Review

Current knowledge of the alkali silica reactions and the use of lithium compounds to mitigate ASR damage, as well as prior research examining the effects of lithium compounds on cement and concrete behavior are reviewed in detail in this chapter.

2.1 ASR Reactions and Mechanisms of Damage

Alkali silica reaction (ASR) occurs when sufficient alkalis, reactive siliceous aggregate, and moisture are present in concrete. Alkalis in the pore solution of concrete, predominantly sodium (Na^+) and potassium (K^+), most often come from the cement, but may also come from supplementary cementitious materials, aggregates, and chemical admixtures. In addition, external sources, such as sea or groundwater, or chemicals applied to the hardened concrete, may contribute alkalis. Repeated exposures to de-icing chemicals are known to contribute to high alkali concentrations in concrete (Rangaraju, 2005).

Mineral components in aggregates that are susceptible to ASR typically have amorphous, poorly crystalline microstructures. Lists of rocks and minerals that are often reactive are available (Folliard et al., 2005; Kosmatka, 2005). Determining the reactivity of an aggregate, however, is not as simple or straightforward as classifying the rock or mineral type. Aggregate reactivity typically must be determined experimentally by procedures such as ASTM C 1260 Standard Test Method for Potential Alkali Reactivity of

Aggregates (Mortar-Bar Method) and ASTM C 1293 Standard Test Method for Determination of Length Change of Concrete Due to Alkali-Silica Reaction.

Researchers generally agree that the alkali silica reaction occurs when hydroxyl ions associated with the alkalis in the pore solution of a concrete penetrate the structure of a reactive aggregate and initiate an acid-base reaction with silinol or siloxane (or simply silica) groups within the aggregate. The resulting silicates eventually combine with alkali cations, and potentially other species, in the pore solution to form an alkali-silica gel. Though there is general agreement that expansion of this alkali-silica gel, as it absorbs water, is the direct cause of the cracking associated with ASR, there is some disagreement on the structure of this gel and the mechanism of this expansion (Folliard et al., 2005; Lumley, 1997).

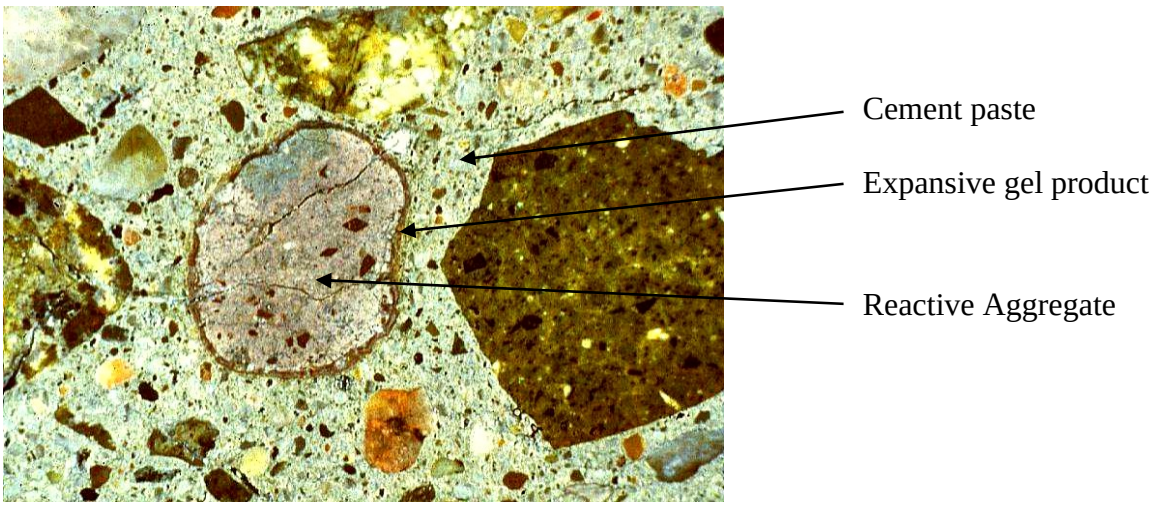

Figure 2.1: ASR reaction product in concrete. (image source: Portland Cement Association (PCA))

2.2 Prevention of ASR Damage in New Concrete Construction

Though strategies exist for rehabilitation of ASR-damaged concretes, including rehabilitation damaged airfield pavements by application of lithium solutions, this research covers lithium use in fresh concrete mixes, and the literature review only covers ASR-mitigation strategies in new construction.

2.2.1 Materials Selection for ASR mitigation

Typical measures taken to prevent ASR damage include use of low alkali cement, reduction in cement content, use of aggregates that have been shown to be non-reactive, and design and detailing to prevent unnecessary exposure to moisture. Use of supplementary cementitious materials (SCMs), particularly Class F fly ashes, has also been shown to decrease ASR-induced expansion. However, recent cases of ASR damage, particularly in airfield pavements, indicate that current measures may not be sufficient. Although lab tests indicate that the use of low alkali cements is effective in preventing ASR-associated expansion, field structures made from comparable low alkali cements at low water-to-cementitious materials ratios have displayed ASR damage, particularly when exposed to external alkalis such as de-icing chemicals. Additionally, structures made using aggregates that were previously thought to be non-reactive have exhibited ASR damage (Folliard et al., 2005). Also, in some more reactive aggregates, ASR cannot be sufficiently limited by traditional methods such as inclusion of SCMs (Thomas et al., 2001). Recent ASR damage, new knowledge on reactivity of aggregates, increasing demand for concrete materials, and relative scarcity of non-reactive aggregates have

prompted research on alternative methods of preventing ASR damage in concrete structures.

2.2.2 Lithium-containing admixtures for ASR mitigation

For over 50 years, lithium compounds have been known to reduce expansion caused by ASR in laboratory specimens (McCoy and Caldwell, 1951). There are several schools of thought on the mechanisms involved, but there is general agreement among researchers that the alkali silica reaction product formed when lithium is present is non-expansive, and thus not deleterious (Folliard et. al., 2005).

Data from the original work by McCoy and Caldwell demonstrating the beneficial effects of lithium on ASR expansion in laboratory specimens is shown in Figure 2.2. Since this effect was demonstrated, substantial work has been done on determining the optimal dosage of lithium in concrete for ASR mitigation. The ratio of lithium to cement total alkali equivalent appears to be the dominant criteria for effectiveness at ASR mitigation (Lumley, 1997). The work of a number of researchers, including Thomas et al.(2000), Durand (2000), Collins et al. (2004), and Tremblay et al. (2004), has led to the adoption of a standard lithium-to-alkali molar ratio of 0.74 as an accepted lithium nitrate dosage, effective in suppressing expansion in laboratory specimens.

A variety of lithium compounds, including lithium fluoride (LiF), lithium chloride (LiCl), lithium bromide (LiBr), lithium hydroxide (LiOH), lithium nitrate ($LiNO_3$), lithium nitrite ($LiNO_2$), lithium carbonate (Li_2CO_3), lithium sulfate (Li_2SO_4), lithium hydrogen phosphate (Li_2HPO_4), and lithium silicate (Li_2SiO_3), have been considered over years of laboratory studies on alkali-silica reaction. Of these, $LiNO_3$ has shown the most promise

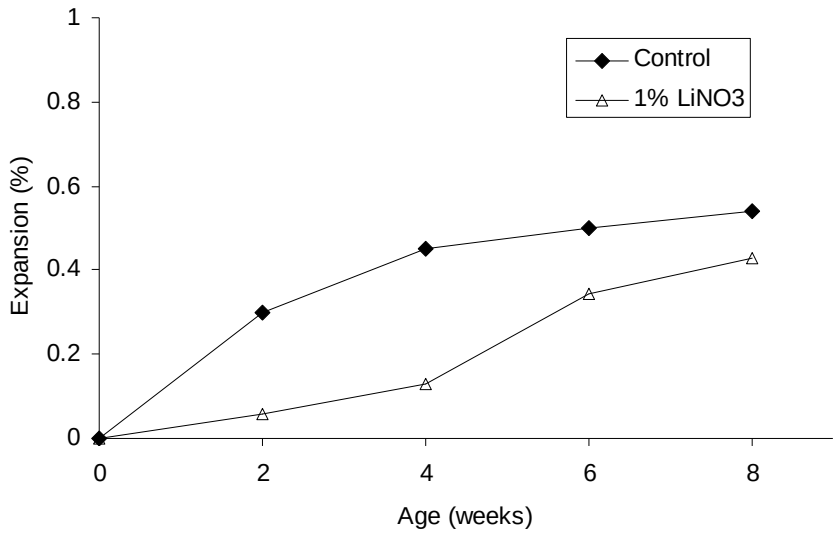

Figure 2.2. McCoy and Caldwell (1951) data showing reduction in ASR expansion in Pyrex glass mortar bar specimens made with lithium nitrate; Li/(Na+K) molar ratio was 0.39.

for practical use for a number of reasons. LiOH and other lithium compounds can increase the hydroxyl ion (OH^-) concentration in the pore solution (increasing the pH), an effect that increases the dissolution of silica groups within the aggregate, increasing the risk of ASR (Diamond and Ong, 1992). When some lithium compounds, such as LiOH, Li_2CO_3, and LiF, are used in insufficient dosages, their use may actually increase expansion by ASR, rather than reduce it – a "pessimum effect" (Stark et al., 1993; Thomas et al., 2000; Diamond and Ong, 1992; Diamond, 1999). Additionally, some lithium salts, such as LiF and Li_2CO_3, are poorly soluble, making them less suitable for use in concrete mixtures. $LiNO_3$ does not increase the pore solution pH, does not exhibit a pessimum effect, and has been shown to be more effective than other lithium compounds in controlling expansion in very reactive aggregates (Stokes et al. 1997). Additionally, the pH of a typical lithium nitrate solution for use as a concrete admixture is around 7 to 9, relatively close to neutral.

This makes lithium nitrate safer to handle that other lithium compounds. Due to these advantages, $LiNO_3$ is the most common active component in commercially available, lithium-containing liquid chemical admixtures for control of expansion associated with ASR.

2.3 Effects of Lithium Admixtures on Early Age Concrete Behavior

While the beneficial effects of lithium in mitigating expansion by ASR have been examined extensively, little research has been done to specifically examine the effects of lithium admixture use on other concrete properties. Rather, information noting the effects of lithium admixtures on concrete properties has been included occasionally in the literature, as periphery information, rather than as the focus of a research effort. The following sections present a review which addresses, at least to some extent, the effects of lithium nitrate and other lithium admixtures on the chemistry of the pore solution and hydration products, and on concrete workability, setting time, shrinkage, air content and unit weight, and strength. Much of the research in the literature examines lithium at current typical dosages or lower. One objective of this research is to examine whether an upper dosage limit exists beyond which early age concrete properties begin to become negatively affected. However, data is lacking in the literature in this regard. Also, no data was found in the available literature on the effects of lithium dosages on other early age properties such as finishability and maturity, though these effects are clearly important to consider.

2.3.1 Concrete Pore Solution and Hydration Product Chemistry

It is known that much of the lithium added to ordinary concrete during mixing will become bound in the hydration products. For example, Diamond and Ong (1992) found that 40% of the lithium added to non-reactive mortars was taken up by the hydration products by 1 day of age. Berubé and co-workers (2004) found that only 35% of the lithium, added as $LiNO_3$, remained in the pore solution at 90 days.

Often, lithium is used in combination with pozzolanic materials, such as fly ash, to avoid damage by ASR in new construction. With fly ash concrete, this lithium-binding effect could be exacerbated because the use of fly ash in portland cement-based materials is known to decrease the Ca to Si ratio in the calcium silicate hydrate (or C-S-H), which is the primary strength-giving phase. Class F fly ash, with its lower CaO content, has a greater effect than Class C fly ash on lowering the Ca:Si. A lower Ca:Si in the C-S-H has been shown to increase alkali binding within the cement hydration product. Lithium is also an alkali earth metal, and its binding within the C-S-H structure will also likely be increased in fly ash mixtures where the Ca:Si is decreased (Bhatty and Greening, 1978; Stade, 1989). In addition, there is evidence that the binding of lithium in the cement hydrates may be preferable to binding of Na^+ or K^+ (Collins et al., 2004; Berubé et al., 2004). The net effect of increased Li binding in hydration products would be a reduction in the amount of "free" lithium (that which remains in the pore solution or loosely bound) which is able to participate in reactions to mitigate expansion by ASR and which may affect other plastic and hardened properties of the concrete.

2.3.2 Workability

While workability is commonly measured in the field and the lab by slump, there has been only very limited published research examining workability effects of lithium admixtures. Thomas et al. (2003) measured slump in concrete mixtures with w/cm of 0.35, Type II cement, 13-21% fly ash by weight of cement, and water reducing and air entraining admixtures. A 30% solution of $LiNO_3$ was used at standard dosage rates, based on the alkali contributed by the cement, and also at standard dosage rates with the dosage based on the alkalis contributed by the cement and fly ash. The authors concluded that the effect of the lithium admixture on slump at these dosage rates was insignificant.

Likewise, Sakaguchi (1990) and co-workers also reported no change in mortar flow with the addition of $LiOH \cdot H_2O$ and $LiCO_3$, and no changes in slump of concrete mixtures was noted during extensive examination of LiOH·H2O by the British Research Institute (Hooper et al., 2004).

However, Lumley (1997) remarked that both $LiOH \cdot H_2O$ and $LiCO_3$ produced "noticeable" early stiffening in concrete mixtures prepared at water-to-cement ratios of 0.50 and 0.525, respectively. The stiffening was severe enough to prohibit proper compaction in one case, and subsequent mixtures in Lumley's experimental program were prepared at higher w/c's. The choice of lithium compound appears to be significant, as Lumley reported only minor stiffening in mixtures containing LiF. The use of $LiNO_3$ was not addressed in that research effort.

The effect of LiOH on slump was addressed by Wang et al. (1996) who found that its use could both increase slump when used in combination with ASTM Type A (water-

reducing) and Type D (water-reducing and retarding) admixtures, and could lead to decreased slump when used with cements with high alkali contents. Reduced slump was particularly apparent in cements with alkali equivalents of 0.80 and 1.02% when Type F and Type G admixtures (high range water reducers) were used.

2.3.3 Setting Time

Some researchers have found that lithium admixtures may shorten the time to set in Portland and calcium aluminate cements, while another report suggests that lithium nitrate may have negligible effects on setting. In Portland cement concrete, Thomas et al. (2003) reported setting times to vary by plus or minus 20 minutes, with the addition of $LiNO_3$, suggesting that the lithium addition may have no consistent and discernible effect in practice on setting time. However, it is worth noting that the mixtures examined by Thomas and co-workers all contained fly ash, which may bind lithium, thus decreasing the potential set accelerating effects of the $LiNO_3$.

Shortened setting times have been reported for $LiCO_3$ (Mo, in review; Gajda, 1996) and LiOH (Mo, 2005) when used in Portland cement pastes. For example, Wang et al. (1996) reported setting times shortened by 20-40 minutes when LiOH was used in combination with an ASTM Type A (water-reducing) admixture and by 40 to 90 minutes when used with a Type F (superplasticizing) admixture in mixtures with a water-to-cement ratio (w/c) of 0.33. The effect was exacerbated for those cements with higher alkali contents. The authors suggested that the shortened setting time may be offset by other means, if necessary. However, methods and proportions for achieving equivalent

setting times were not provided, and data for setting time when lithium was used in combination with retarding admixtures was also not reported.

In the most severe case described in the literature, Gajda (1996) reported $LiCO_3$ shortened setting times by a factor of 2 or 3. However, this effect may be due to the poor solubility of $LiCO_3$, which could contribute to early precipitation, and the earlier stiffening and setting observed by Mo (in review) and Gajda (1996). The solubility of $LiNO_3$, the subject of this research, is 850g/L water, (roughly 64 times more soluble than $LiCO_3$, at 13 g/L water) (Lumley 1997). Also, the paste setting times in Mo's studies were already substantially shortened by raising the equivalent alkali content to 3.0%, and the addition of lithium compounds produced only small additional decreases in setting time, when comparing the alkali-loaded samples (both with and without lithium) to the control pastes. However, lithium salts have been shown to act as set accelerators for high-alumina or medium-alumina cements (Novinson and Crahan, 1988), suggesting that some accelerating effect may be possible.

There is also some evidence that the lithium admixture dosage rate may influence setting characteristics. Certain chemical admixtures, such as $CaCl_2$, for example, can act as set accelerators at low dosages and set retarders at higher dosages. Novinson and Crahan (1988) proposed that the concentration of the lithium salt and its effect of pore solution pH (which is related to the anion associated with the lithium) are important factors in determining the effect of lithium addition on setting time.

2.3.4 Shrinkage

To date, Lane (2002) is the only author to address shrinkage in lithium-containing concrete. Lane used a method described in ASTM C 157 to examine shrinkage in 28-day moist-cured air-entrained concrete prisms prepared with w/cm of 0.45 and cement content of 378 kg/m3 at $LiOH \cdot H_2O$ and $LiNO_3$ at 75 and 100% of the standard dosage. One-year shrinkage data, after exposure in a 50% RH environment, showed no difference between the lithium-containing concrete and the ordinary concrete. However, the low cement content in Lane's mixtures could have affected these results, as the paste is the fraction that experiences shrinkage. Tests should be performed at higher cement factors to fully appreciate the effect, if any, of lithium addition on shrinkage.

Shrinkage can be problematic in concrete with a more refined pore structure, where set has been accelerated. Some lithium admixtures are suspected to accelerate setting (Mo, 2004, in review) and perhaps the rate of strength gain (McKeen et al., 2000). Also, concretes with increased alkali contents – and lithium is an alkali – have been shown to be more susceptible to shrinkage cracking (He and Li, 2005).

2.3.5 Air Content and Unit Weight

In addition to slump (described in Section 2.4), air content (most commonly by the pressure method ASTM C 231) and unit weight (ASTM C 138) are generally measured in the field as part of standard quality control. However, little data exists in the literature to describe the effect, if any, of lithium on air content and unit weight.

The effects on unit weight, in particular, have received only scant attention in the literature. Britain's Building Research Establishment (BRE) reports no change in wet

density in concrete mixtures containing $LiOH \cdot H_2O$, as compared to ordinary concrete (Hooper et al., 2001).

The effects of lithium admixture addition on air content, in air-entrained concrete, may be preliminarily examined through work presented by Wang et al. (1996), Lane (2002), and Thomas et al. (2003). Wang et al. (1996) report no significant effect of LiOH use on air-entrainment. The air content of lithium-containing fresh concrete generally deviated little from the control samples. In a study by Lane (2002), concretes were prepared with w/cm of 0.45 with a constant cement content and air entrainment dosage in combination with $LiOH \cdot H_2O$ or $LiNO_3$ at 75 and 100% dosage. An adequate air entrainment system was developed in all samples, providing excellent freeze-thaw resistance, as measured by ASTM C 666 Procedure A (i.e., 98-101). Air contents of 4.2 to 6.1% were achieved in lithium-containing mixtures, compared to 4.0% in the control. Thomas et al. (2003) recorded air contents of 5-7% for air-entrained concretes produced with $LiNO_3$ dosages of 0, 75, and 100% of the standard dosage. However, the dosages of air entraining admixture (AEA) in these lithium-containing concrete mixtures were in some cases up to 50% higher than in the control mixtures. Thomas et al. did not comment on the reasoning or need for higher AEA dosage in these mixtures, and air contents are not provided for many of the mixtures examined. When tested according to ASTM C 666 Procedure A, all of the concretes exhibited high durability factors of 96-99, regardless of the lithium admixture dosage, indicating that a stable and sufficient system of air entrainment was achieved. It is unclear, however, if a higher dosage of AEA was required to achieve the necessary amount of entrained air in the presence of lithium nitrate.

In a recent review on the factors influencing air entrainment in concrete, Du and Folliard (in press) state that many inorganic electrolytes when used as chemical admixtures in concrete can influence the foaming ability of air entraining admixtures. For example, $CaCl_2$, a common set-accelerating admixture, may react with the surfactants in the AEAs to form insoluble precipitates, which decrease their foaming ability. Because of the complex nature of the potential interactions between different chemical admixtures when used in combination, Du and Folliard (in press) suggest that admixture compatibility be examined experimentally.

2.3.6 Strength

The rate of strength development and the strength at early ages are important considerations for planning construction operations. However, the effect of lithium admixtures on strength development has not been well addressed in the published literature. When strength data has been presented, the effect of lithium on compressive strength is reported. While compressive strength is the most common measure of concrete quality in practice, it is less typically used for pavement or airfield construction, where flexural strength development is most relevant. However, no data regarding the effects of lithium on the flexural strength of concrete were found in the literature.

Lithium has been shown by various researchers to have different effects, including no measurable effect as well as both positive and negative effects, on strength. In an investigation of two different concrete mixture designs where the cement content varied, Thomas et al. (2003) found the compressive strengths of lithium-containing concrete (at 75 and 100% of the standard $LiNO_3$ dosages) to be nearly identical to those concretes

without lithium at the ages of 3, 7, 28, 56, and 90 days. Likewise, no detrimental or beneficial effect on strength was reported by Ohama et al. (1990) for mortars containing LiF or Li_2CO_3 and independently by Johnson (1997), Stokes (2001), and Lane (2002) for $LiNO_3$-containing concretes.

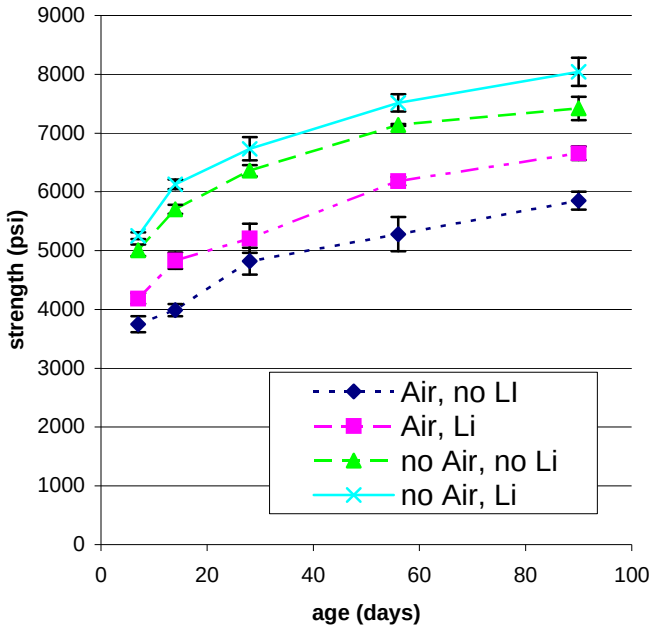

Figure 2.3. Data from McKeen et al. (2000) showing lithium-containing concrete (with and without air entrainment) to exhibit higher compressive strength, although the difference was concluded to not be statistically significant.

While the results of Thomas et al. (2003) suggest no accelerating effect with $LiNO_3$ use, one report suggested that the admixture may act very moderately to increase the rate of strength development. At 75, 100, and 125% of the standard $LiNO_3$ dosages, McKeen et al. (2000) concluded that the admixture-containing concretes generally exhibited higher 7, 14, 28, 56, and 90-day strengths, but that the increases in strength (shown in Figure 2.3) were not statistically significant. Also, it should be noted that the air contents of the lithium-containing concrete were slightly lower than the ordinary

concrete for both the air-entrained (4.0% vs. 6.2%) and non air-entrained (0.9% vs. 1.1%) mixtures which could be responsible for the higher observed strength.

While strength was generally not affected by the use of LiOH in concrete examined by Wang et al. (1996), in some cases compressive strength was negatively affected, as shown in Figure 2.4. In particular, in high alkali cements (e.g., Na_2O_e of 0.80% or more in Wang et al.'s study), 28-day compressive strength was reduced by as much as 25% in the presence of lithium, although often 1-day strengths were greater than the control concretes. Also, concretes prepared with lower alkali cements showed equivalent or even higher compressive strength in the presence of lithium, suggesting that the detrimental effect on strength may be linked to the cement alkali content for $LiNO_3$.

Tests performed by BRE (Figure 2.5) also indicated that reductions in 28-day compressive strength are possible in concrete containing $LiOH \cdot H_2O$ (Hooper et al., 2004). Lane (2002) also concluded that compressive strength was decreased when $LiOH \cdot H_2O$ was used at a 100% dosage rate. Also, as stated previously, Mo (2005) reported that compressive strength of mortars decreased with increasing LiOH content, and the rate of strength developed seemed to lag behind control mixtures. However, mortar flexural strength was relatively unaffected by lithium hydroxide addition. These data support Wang et al.'s (1996) observation that $LiOH \cdot H_2O$ can act as a hydration retarder.

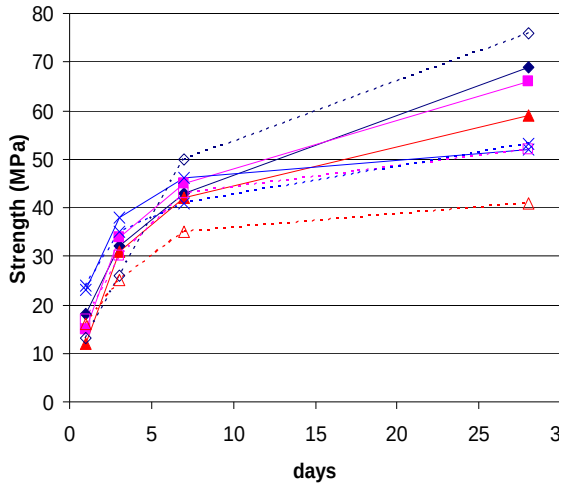

(a) Type A admixture

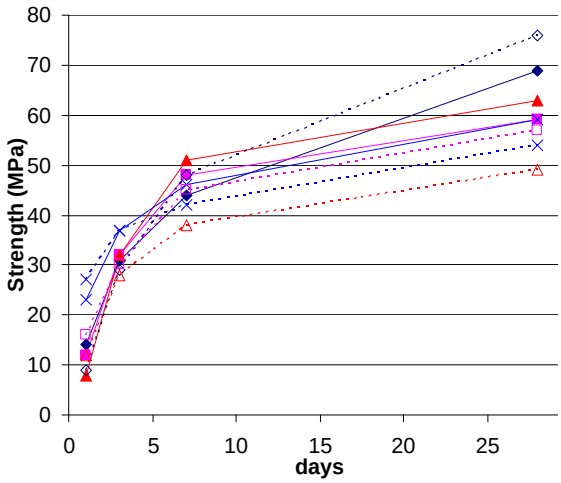

(b) Type D admixture

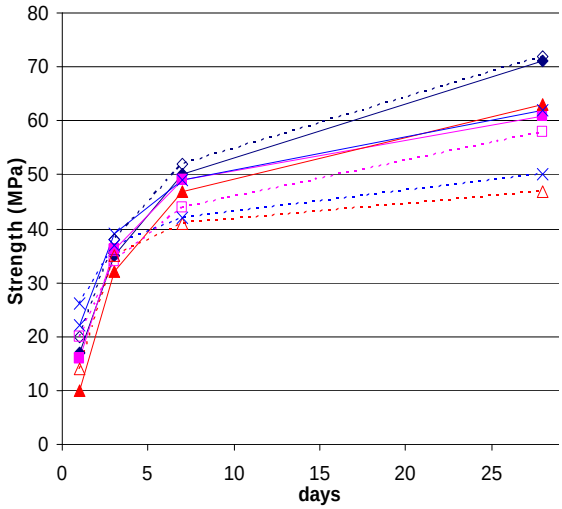

(c) Type F admixture

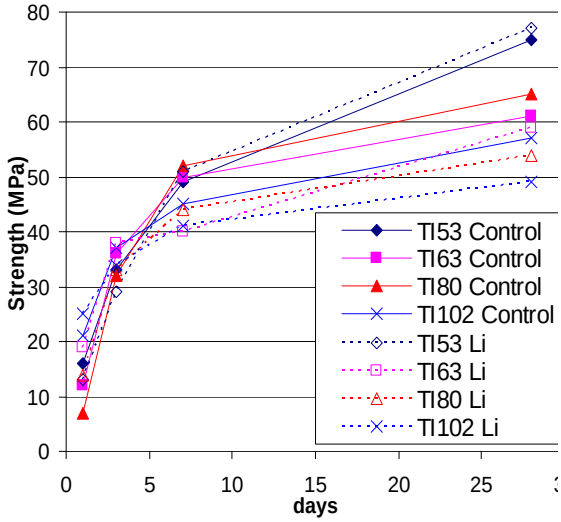

(d) Type G admixture

Figure 2.4. In research investigating potential interactions between LiOH admixture and ASTM Type A, D, F, and G admixtures, compressive strength was found to generally be reduced when lithium was used in mixtures with higher alkali cements. The cement alkali content is noted in the legend as the last two digits in the sample type designation (e.g., TI53 cement has a total equivalent alkali content of 0.53% and TI102 has 1.02%). Data are from Wang et al. (1996).

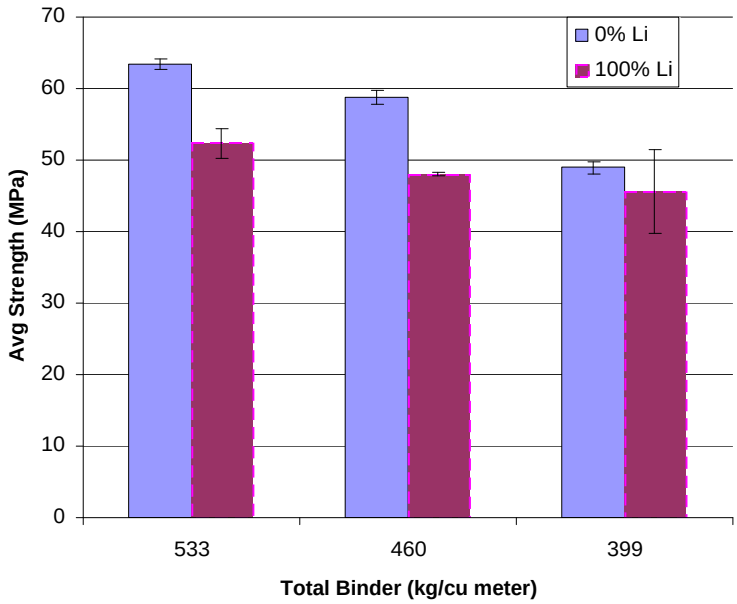

Figure 2.5. Hooper et al. (2004) report lower 28-day concrete compressive strength at 100% $LiOH \cdot H_2O$ dosage in samples prepared and monitored by BRE.

CHAPTER III

Materials and Experimental Methods

The purpose of this research is to holistically examine potential effects of $LiNO_3$, at 0, 50, 100, 200, and 400% of the standard dosage, on early age concrete behavior. The effects of $LiNO_3$ addition rate on six different cements, which vary primarily in their alkali content and C_3A content, were examined. Additional testing was performed on a single cement, again with varying $LiNO_3$ dosage, where 20% Class F fly ash was included. Details regarding the materials and test methods employed are described herein.

3.1 Materials

Lithium nitrate is of particular interest in airfield pavements. Mix proportions and materials used in this research were chosen to simulate airfield pavement concrete. Mix proportions for lab testing were based on the mix design used for concurrent reconstruction of Ramps 1 and 3 at Hartsfield-Jackson Atlanta International Airport. In laboratory tests on concrete, aggregates and admixtures and their proportions were the same as those used in the airport reconstruction project. In laboratory tests on cement paste, the water-to-cement ratio of 0.30 was based on this mix design. Additionally, the cement tested with and without Class F fly ash replacement, as well as the fly ash, were the same as those used in the airport reconstruction project, and with the same 20% replacement amount.

3.1.1 Cementitious Materials

Since common cement alkalis (sodium and potassium) are known to affect the rate of the tricalcium aluminate (C_3A) reactions during cement hydration, it is reasonable to expect that lithium (also an alkali) may also affect this balance. Therefore, cements with a range of tricalcium aluminate contents were included in this research. Additionally, work by Wang et al. (1996) has suggested that the behavior of cements with different alkali contents are affected differently by lithium compounds. Therefore, cements with varying alkali contents were also examined. Though the selection of cements was limited by commercial availability, effort was made to select a matrix of cements that allowed comparison of behavior at differing values of these particular variables (alkali content and C_3A content.)

The six different cements used in testing lithium nitrate effects are shown with oxide analysis and Bogue potential compositions in Table 3.1. Table 3.2 shows three of these cements chosen to examine lithium nitrate's effects on cements of varying alkali contents. Table 3.3 shows three of the cements chosen to examine lithium nitrate's effects on cements of varying tricalcium aluminate contents. Although these cements were chosen to minimize differences in other component contents, it is clear that other variables exist when making comparisons between effects on these cements.

Since Class F fly ash is known to have positive effects on ASR durability, it is reasonable to expect lithium-containing mixes to also contain Class F fly ash. Since lithium may be bound into the C-S-H structure to a greater extent in Class F fly ash mixes, it is likely that lithium will affect these mixes differently than an ordinary Portland

cement concrete mix. Cement 6, the cement used in the Hartsfield-Jackson Atlanta International Airport Ramps 1 and 3 reconstruction project, was tested with and without 20% Class F fly ash replacement, in order to investigate fly ash effects. The composition of Cement 6 and the Class F fly ash used are shown in Table 3.1. Table 3.4 shows the mix design used in the Hartsfield-Jackson Atlanta International Airport Ramps 1 and 3 reconstruction project, which was the basis for mix proportions in this research.

Table 3.1: Oxide analysis and Bogue potential compositions for cements and fly ash.

	Cement 1	**Cement 2**	**Cement 3**	**Cement 4**	**Cement 5**	**Cement 6**	**Class F Fly Ash**
	Low alkali	Moderate Alkali & C3A	High alkali	Low C3A	High C3A	Airport	Project
SiO_2 (%)	20.44	20.98	20.13	21.00	19.29	20.06	50.77
Al_2O_3 (%)	5.24	4.72	5.48	3.62	5.62	4.89	19
Fe_2O_3 (%)	3.99	2.99	3.26	3.47	2.82	3.00	17.72
CaO (%)	63.22	63.56	60.93	62.52	64.21	64.22	5.1
MgO (%)	1.05	2.24	2.45	4.29	0.86	2.68	0.91
SO_3 (%)	3.74	2.61	4.00	2.43	3.54	2.74	1.56
Na_2O (%)	0.069	0.165	0.344	0.231	0.257	0.115	0.65
K_2O (%)	0.343	0.523	0.866	0.404	0.464	0.444	2.31
NaO_2 Equiv. (%)	0.295	0.509	0.91	0.50	0.562	0.407	2.17
P2O5 (%)	0.092	0.335	0.157	0.054	0.256	0.076	0.12
TiO_2 (%)	0.318	0.241	0.214	0.172	0.614	0.274	1.08
SrO (%)	0.065	0.035	0.194	0.050	0.231	0.038	0.04
Mn_2O_3 (%)	0.079	0.150	0.173	0.064	0.040	0.088	0.05
Cr_2O_3 (%)	0.012	0.008	0.025	0.005	0.014	0.012	
LOI (%)	1.33	1.44	1.78	1.69	1.79	1.37	0.62
C_3S (%)	50.4	55.9	42	59	62.9	64.1	NA
C_2S (%)	20.6	18.0	26	16	7.9	9.2	NA
C_3A (%)	7.1	7.5	9	4	10.1	7.9	NA
C_4AF (%)	12.2	9.1	10	11	8.6	9.1	NA
Blaine Fineness (m2/kg)	380	369	376	370	368	345	161

Table 3.2: Cements used for alkali range comparison

	Cement 1 **Low Alkali**	**Cement 2** **Moderate Alkali**	**Cem,ent 3** **High Alkalli**
Na_2O (%)	0.069	0.165	0.344
K_2O (%)	0.343	0.523	0.866
NaO_2 Equiv. (%)	0.295	0.509	0.91
C_3S (%)	50.4	55.9	42
C_2S (%)	20.6	18.0	26
C_3A (%)	7.1	7.5	9
C_4AF (%)	12.2	9.1	10

Table 3.3: Cements used for C_3A range comparison

	Cement 4 **Low C3A**	**Cement 2** **Moderate C3A**	**Cement 5** **High C3A**
Na_2O (%)	0.231	0.165	0.257
K_2O (%)	0.404	0.523	0.464
NaO_2 Equiv. (%)	0.50	0.509	0.562
C_3S (%)	59	55.9	62.9
C_2S (%)	16	18.0	7.9
C_3A (%)	4	7.5	10.1
C_4AF (%)	11	9.1	8.6

Table 3.4. Production mix proportions in use at the Hartsfield-Jackson Atlanta International Airport. Note: Water amount shown requires reduction for water in lithium nitrate admixture, as shown in Section 3.1.2.

Material	Quantity/yd^3	
Cement 6 (Type 1)	611	lb
Class F fly ash	153	lb
Water	230	lb
Florida Rock #4 Crushed Stone	618	lb
Florida Rock #67 Crushed Stone	1444	lb
MM-Shorter Natural Sand	920	lb
AEA-92 Air Entraining Agent	4.5	fl oz
Eucon NR water-reducer / retarder	15.28	fl oz
Plastol 341 plasticizer	30.56	fl oz
Lithium Admixture	(varying dosages)	

3.1.2 Lithium Admixture

Lithium nitrate ($LiNO_3$) was selected for this research, since it is currently the most commonly used lithium compound for ASR suppression. The lithium nitrate admixture used in this research is FMC Lithium's Lifetime N Admixture, an approximate 30% by weight $LiNO_3$ solution in water, CAS No. 7790-69-4. At 25 degrees Celsius, the density of this solution is 10.0 lb/gallon (1.20 g/cm^3). The particular batch that was used was tested at 30.5% $LiNO_3$ by weight.

Lithium admixture dosages, by current methods, are based on optimal suppression of ASR expansion. The standard dosage for a concrete mix is a function of the alkali content of the cement being used. Previous research has led to establishment of a standard optimal dosage of 0.74 lithium-to-alkali molar ratio (Folliard, 2005). The quantity of alkali present in a cement is typically expressed as total sodium oxide equivalent (Na_2O_e), or "equivalent soda", and is a weighted combination of sodium oxide (Na_2O) and potassium oxide (K_2O). In terms of percent by weight:

$$\%Na_2O_e = \%Na_2O + 0.658\ \%K_2O$$

The weight of equivalent alkali in a concrete batch is:

$$\text{weight of } Na_2O_e = (\text{weight of cement in batch}) \times (\%Na_2O_e)/100\%$$

The weight of lithium nitrate required to achieve the standard dosage of 0.74 lithium-to-alkali molar ratio can be calculated by multiplying the weight of alkali equivalent in a

batch by the ratio of molecular weights of $LiNO_3$ and Na_2O (dividing the latter by two since sodium oxide contains two Na ions) and multiplying by the desired molar ratio of 0.74. For a concrete batch with one pound of total alkali, the dosage would be:

$$1 \text{ lb } Na_2O_e \times \left(\frac{68.94 \text{ lb } LiNO_3}{61.98 \text{ lb } Na_2O_e / 2} \right) \times 0.74 = 1.65 \text{ lb } LiNO_3/\text{lb } Na_2O_e$$

To calculate the volume of 30% by weight $LiNO_3$ admixture required, this 1.65 lb $LiNO_3$ is divided by the weight fraction of $LiNO_3$ in the admixture (0.30), and then by the solution density (10.0 lb/gallon):

$$(1.65 \text{ lb } LiNO_3) / (0.30) / (10.0 \text{ lb/gallon}) = 0.55 \text{ gallons } LiNO_3 \text{ admixture}$$

This dosage, corresponding to the 0.74 lithium-to-alkali molar ratio established by previous researchers, is the basis for the manufacturer's recommended dosage: "For every pound of Na_2O_e present… you need 0.55 gallon of Lifetime N" (FMC Lithium).

For the purpose of this research, this standard dosage of 0.74 lithium-to-alkali molar ratio, corresponding to 0.55 gallon of Lifetime N per lb of total cement alkali, is referred to as the 100% dosage for a given cement. This 100% dosage is then greater for a concrete mix using a higher alkali cement, and lower for a concrete mix using a lower alkali cement. For each set of experiments, a 0% dosage mix is examined as a control mix, with no lithium nitrate admixture. 400% lithium nitrate dosage mixes represent mixes made using four times the standard dosage for the cement being examined.

Lithium nitrate dosages evaluated in most sets of experiments include 0%, 50%, 100%, 200%, and 400%.

The manufacturer (FMC Lithium) recommends a reduction of water in the mix design of a concrete with lithium nitrate admixture to compensate for the 70% weight fraction of water in the admixture. The recommended water reduction is 0.85 gallon for every gallon of admixture added. This is approximately equal to the admixture density, multiplied by the weight fraction of water in the admixture (0.70), and divided by the density of water:

$$\left(\frac{10\,\text{lb}}{\text{gallon admixture}}\right)\times\left(\frac{0.70\,\text{lb water}}{\text{lb admixture}}\right)\times\left(\frac{\text{gallon}}{8.33\,\text{lb}}\text{water}\right) = 0.84 \text{ gallon water reduction per gallon admixture added.}$$

All mixes in this research were adjusted to compensate for this water in the admixture, using a volumetric water reduction factor of 0.833, rather than the manufacturer's recommended 0.85. This factor of 0.833 more closely accounts for the water in the particular batch of admixture used, which has known weight fractions 30.5% $LiNO_3$ and 69.5% water.

3.2 Experimental Methods

Table 3.5 summarizes the number of specimens at each dosage and for each cement, for each of the tests performed. Isothermal calorimetry provided information on heat generation during hydration, and was interpreted to make conclusions on rates of reaction and extent of reaction. Measures of concrete workability are of great practical

importance to understanding lithium effects on concrete behavior. Slump measurements and rheology testing were employed to make conclusions on lithium effects on concrete flowability, and bleed water testing was employed to examine any lithium effect on the amount of bleed water. Vicat time of setting tests were utilized to examine lithium effects on initial and final set of cements. Chemical shrinkage tests were used not only to examine shrinkage of a cement paste, but also to make conclusions on extent of reaction. Autogenous shrinkage testing provided an understanding of post-final-set linear shrinkage, an appropriate measure for making conclusions on shrinkage that could cause cracking. Free shrinkage (performed after 24 hours of age) and restrained shrinkage testing provided similar information relative to the resistance to cracking. These two tests have the advantage of inclusion of the restraining effects of aggregates, and the drying component of shrinkage. Larger variation was expected, however, due to the inclusion of the aggregates. Finally, analysis of results of strength testing provided information on lithium effects on concrete flexural and compressive strength.

Table 3.5. Test methods and numbers of specimens

Test	Number of Cements*	Number of Dosages	Specimen per case	Total Specimens
Calorimetry	7	5	1	35
Rheology	1	3	3	9
Slump (ASTM C 143)	1	3	1	3
Bleed Water (ASTM 232)	2	3	1	6
Vicat Time of Set (ASTM C 191)	7	3 to 5	3	75
Vicat Time of Set at Elevated Temp	2	5	3	30
Chemical Shrinkage (ASTM C 1608)	7	3 to 5	3	75
Autogenous Shrinkage	7	3 to 5	3	75
Free Shrinkage (ASTM C 157)	2	5	3	30
Restrained Shrinkage (ASTM C 1581)	2	5	1	10
Compressive Strength (ASTM C 39), field	1	5	10	50
Compressive Strength (ASTM C 39), lab	1	5	5	25
			Total number of specimens	423

* Cement 6 with 20% Class F fly ash replacement is counted as a separate cement case in this column.

3.2.1 Isothermal Calorimetry

Isothermal calorimetry provided heat of hydration data, measured over time, for a hydrating cement paste specimen. A 3114 TAM Air Isothermal Calorimeter (Figure 3.1) with 8 channels and data logger was used to measure heat of hydration in paste specimens at 0%, 50%, 100%, 200%, and 400% $LiNO_3$ dosages, for each of the cements in Table 3.1, as well as Cement 6 with 20% Class F fly ash replacement.

Prior to mixing, the cement, fly ash, lithium nitrate solution, and de-ionized water were stored at 25 degrees Celsius and 50% relative humidity in environmental chambers for 48 hours to minimize initial differences between paste specimens. For the duration of the project, the temperature in the environmental chambers used to pre-condition materials and to control specimens was observed to fluctuate within a range of 24.5$\pm$0.4 degrees Celsius, and relative humidity was observed to fluctuate between 47 and 51%.

Figure 3.1. 3114 TAM Air Isothermal Calorimeter

Batches of 0.45 lb of paste were mixed at a water-to-cementitious material ratio of 0.30. Before mixing the cement and water, the water and $LiNO_3$ solution were first stirred together in a 300 mL plastic beaker. For mixes involving fly ash, the fly ash and cement were also first blended together by stirring for 60 seconds. The cement was then added to the water/$LiNO_3$ solution in the plastic beaker. The paste was stirred by hand for 10 seconds, and then mixed for 50 seconds using an electric hand mixer.

After mixing, paste quantities of approximately 5 grams each were placed in 20 mL plastic ampoules, which were inserted into the calorimeter at a time of 6 minutes after initial water-cement contact.

Heat generation data were recorded every 60 seconds for 72 hours for each paste specimen. The calorimeter maintained the specimens at a temperature of 25 degrees Celsius.

3.2.2 Rheology and Slump

Effects of lithium nitrate on concrete workability were investigated using slump and rheology testing. Slump testing was performed in accordance with ASTM C 143-05, Standard Test Method for Slump of Hydraulic-Cement Concrete. While widely used due to its simplicity, the slump test does not provide complete information on the flow behavior of concrete. Generally, the flow behavior of concrete approximates that of a Bingham fluid. An ideal Bingham viscoplastic material behaves as a solid at stresses below a yield stress, and flows as a viscous liquid above that yield stress. Two parameters, a yield stress and a viscosity above that yield stress, are necessary to characterize a Bingham fluid. The rheometer used in this research, shown in Figure 3.2,

is a BT-2 two-probe rheometer, and measures torque on two probes as the device is rotated through a pan of fresh concrete. Since the probes are at different radii from the center of rotation, the measurements provide data at two different speeds. This allows a representation of shear stress and strain rate at two points. Because there is currently not a standard test method for measuring rheology parameters in absolute terms, the shear stress and strain rate values are expressed as torque and speed, respectively, and the slope of a line fit to this data represents *relative* viscosity. The y-intercept of this line, then, represents the *relative* Bingham yield stress in terms of torque. Testing with the rheometer has the advantage of providing measures of two parameters, while the slump test provides only a measure, which is dependent on the yield stress. While the relative Bingham yield stress and the slump of the concrete are essentially measurements of the same parameter, there is currently not an absolute standard, or method to allow direct comparison of the two measures.

Effects of $LiNO_3$ dosages of 0%, 100%, and 400% were tested in fresh concrete made from Cement 6, with no Class F fly ash. For each dosage, one batch was mixed, and one slump measurement was recorded. For each of these mixes, three measurements were taken with the rheometer.

Figure 3.2. Two-probe BT-2 Rheometer for modified two-point test

Mix proportions for these tests were not representative full scale batches currently in production at the Hartsfield-Jackson Atlanta International Airport for several reasons. First, initial slump testing using the H-JAIA mix design led to slump measurements of less than ¼ inch. With measurements this small, there was no observable difference in slump between the dosages tested. However, it was considered that at higher water-to-cement ratios, lithium nitrate may have an effect. The second reason for using a different mix design is that based on prior experience with the rheometer, repeatable results were more achievable using mixes with higher slumps. Hence, a water-to-cement ratio of 0.45 was used in mixing the concrete for these tests. Mix proportions are shown in Table 3.6. In lithium-containing batches, the amount of water given in the table was reduced to account for the water in the lithium admixture, as described in Section 3.1.2. Mixing

procedure was consistent with ASTM C 192-05, Standard Practice for Making and Curing Concrete Test Specimens in the Laboratory.

Table 3.6. Mix proportions for slump and rheology testing.

Material	Quantity
Cement	25.93 lbs
Water	11.67 lbs
Coarse Aggregate	55.56 lbs
Fine Aggregate	53.15 lbs
$LiNO_3$ admixture	(variable based on dosage)

3.2.3 Bleeding

Effects of lithium nitrate on the relative quantity of mixing water that will bleed from a fresh concrete was investigated by ASTM C 232-04, Standard Test Method for Bleeding of Concrete. Effects of lithium nitrate on bleeding were examined using Cement 6, both alone and with 20% replacement by Class F fly ash, at a water-to-cementitious material ratio of 0.30. Lithium was dosed at 0%, 50%, 100%, 200%, and 400% for both of these cement cases.

Coarse and fine aggregates were used at the same proportions as full scale batches currently in production at the Hartsfield-Jackson Atlanta International Airport shown in Table 3.4, including the #4 coarse aggregate (which was replaced by #67 aggregate in some lab tests). Mixing procedure was consistent with ASTM C 192-05, Standard Practice for Making and Curing Concrete Test Specimens in the Laboratory. After the fresh concrete was placed in steel cylindrical containers, the concrete surface was levelled and smoothed so that bleed water could be identified and drawn off. Considerable work was required to smooth the surface of the stiff mix, and trowels were

used dry, to prevent introduction of surface water that might be mistaken for bleeding. The containers were covered using plastic wrap and then a bucket lid, to prevent evaporation between periodic checks for bleed water.

3.2.4 Vicat Time of Setting

Time of setting of cement pastes at room temperature with varying $LiNO_3$ dosages were measured, following ASTM C 191-04b Standard Test Method for Time of Setting of Hydraulic Cement by Vicat Needle. Vicat setting times for three paste specimens at each of the $LiNO_3$ dosages of 0%, 50%, 100%, 200%, and 400% were measured for Cement 6, both with and without 20% fly ash replacement. Three paste specimens at each of the $LiNO_3$ dosages of 0%, 100%, and 400% were tested for the remainder of the cements in Table 3.1.

Prior to mixing, cement, fly ash, lithium nitrate solution, and de-ionized water were stored at 25 degrees Celsius and 50% relative humidity in environmental chambers for 48 hours to minimize initial differences between paste specimens.

Paste batches of 7 lb each were mixed with water-to-cementitious material ratio of 0.30. A w/cm of 0.30 was chosen to minimize bleeding and to provide continuity between the different cement pastes examined, and to as closely as possible simulate the Hartsfield-Jackson Atlanta International Airport reconstruction mixes. The procedure for mixing of each paste followed ASTM C 305-99, Standard Practice for Mechanical Mixing of Hydraulic Cement Pastes and Mortars of Plastic Consistency, with two modifications. First, the lithium nitrate solution was stirred into the water in the mixing bowl before the cement was added. Secondly, mixing was paused twice during the

prescribed 90 seconds for scraping paste down from the sides of the bowl, rather than once, as ASTM C 305 instructs. These were the only deviations from ASTM C 305-99.

The mixed pastes were molded into 3 Vicat specimens per batch, and sealed in plastic containers containing wet sand to provide humidity. Periodically, the specimens were removed, and a Vicat apparatus (Figure3.3) was used to measure the penetration of a 1-mm Vicat needle into the paste. ASTM C 191-04b defines initial setting time as the time elapsed between initial water/cement contact and the time when the penetration is 25 mm. Final set is designated as the time when the needle no longer leaves a complete circular impression on the paste surface.

Since concrete curing temperatures are likely higher than room temperature, particularly in pavements in hot locations such as Hartsfield-Jackson Atlanta International Airport, time of setting tests were also performed at an elevated temperature of 35 degrees Celsius. These Vicat tests were performed in triplicate, using Cement 6 with and without 20% fly ash replacement, with $LiNO_3$ dosages of 0%, 50%, 100%, 200%, and 400%.

For these elevated temperature Vicat tests, the humid containers for the specimens were kept in an oven at 35 degrees Celsius for 24 hours preceding the testing, and remained in the oven during testing. These containers contained wet coarse aggregate, for the purpose of maintaining both high humidity and elevated temperature. In order to maintain heat and humidity, these containers were removed from the oven and opened only for periodic measurements.

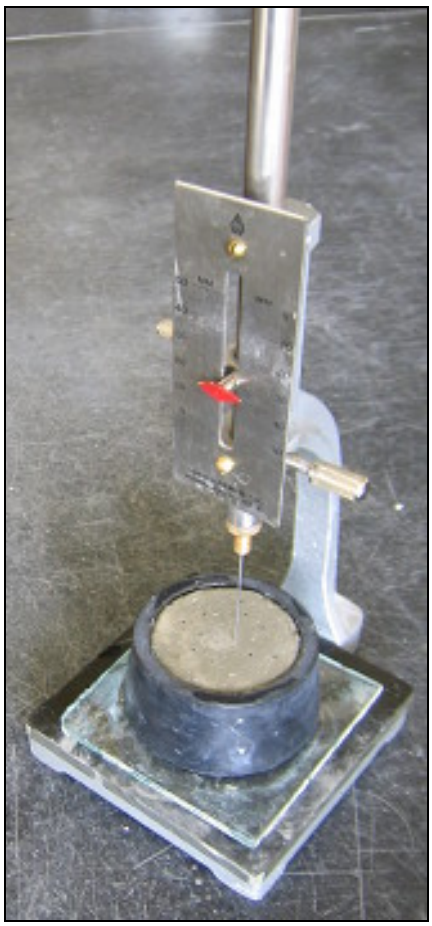

Figure 3.3. Vicat time of setting apparatus

Figure 3.4. Specimen storage container for elevated-temperature time of setting test.

3.2.5 Chemical Shrinkage

Chemical shrinkage is the absolute (internal) volume change accompanying cement hydration and is due to hydration products occupying less physical volume than the reactants. ASTM C 1608-05, the Standard Test Method for Chemical Shrinkage of Hydraulic Cement Paste, was followed to measure chemical shrinkage in 75 paste specimens. ASTM C 1608-05 describes a procedure in which a specimen of cement paste, in contact with a layer of water, is isolated in a glass vial with a pipette (Figure 3.5). As the internal volume of the hydrating cement decreases, water is pulled into the paste, and the associated volume change is recorded from graduations on the pipette. Because water must be able to permeate the paste in this test, there is concern that low

water-to-cementitious material ratios may be inappropriate. Rather than the 0.30 ratio used for other tests in this research, a water-to-cementitious material ratio of 0.40 was used in the pastes for the chemical shrinkage tests.

Figure 3.5. Chemical shrinkage specimens

Triplicate paste specimens were measured for Cement 6 with and without 20% fly ash replacement, at $LiNO_3$ dosages of 0%, 50%, 100%, 200%, and 400%. Triplicate specimens were measured at $LiNO_3$ dosages of 0%, 100%, and 400% for the remainder of the cements in Table 3.1.

Prior to mixing, de-ionized water for mixing the pastes was de-aerated. This was done by boiling the water in a microwave for 5 minutes and by then sealing the water in a rigid polycarbonate container as it cooled. The water container was then stored, along with the cement, fly ash, and lithium nitrate solution, in an environmental chamber at 25 degrees Celsius and 50% relative humidity for 48 hours to minimize initial differences before the paste was mixed.

Paste batches of 0.45 lb were mixed at the ASTM C 1608-specified water to cementitious material ratio of 0.40. The water and $LiNO_3$ solution were first stirred together in a 300 mL plastic beaker. For mixes involving fly ash, the fly ash and cement were first blended together by stirring for 60 seconds. The cement was then added to the water/$LiNO_3$ solution in the plastic beaker. The paste was stirred by hand for 10 seconds, and then mixed for 50 seconds using a Sunbeam model 2470 electric household mixer.

After mixing, paste quantities of approximately 5 grams each were placed in glass vials, and the vials were vibrated for 30 seconds. Three grams of the de-aerated water were then carefully added to the top of the paste. The remainder of the vial was carefully filled with hydraulic oil. A stopper with a 1.0 mL pipette inserted was used to seal the vial so that the oil level in the pipette indicated an initial aggregate volume for the three-phases in the vial. The vials were then allowed to reach equilibrium in the temperature-controlled chamber for 30 minutes before initial readings were recorded. Subsequently, volume change readings were recorded with the vials remaining in the chamber, for 28 days.

The setup described in ASTM C 1608-05 uses water to fill the vial, and then a small amount of oil in the pipette. In this research, added water was limited to three

grams in order to lessen the leaching of lithium ions from the paste into the water. This was the only significant deviation from the ASTM C 1608-05 procedure.

For the duration of the project, the temperature in the environmental chambers used to condition materials and to control specimens was observed to fluctuate within a range of 24.1 to 24.9 degrees Celsius, and relative humidity was observed to fluctuate between 47 and 51%.

3.2.6 Autogenous Shrinkage

Autogenous shrinkage is a measured linear deformation, measured after final setting, in a sealed paste specimen. This shrinkage is largely due to tensile forces in the paste's capillary pore network due to self desiccation of the hydrating cement. A method described by Jensen and Hansen (1995) was used to measure autogenous shrinkage in this research. In Jensen and Hansen's method, cement paste specimens are sealed in flexible corrugated plastic tubes that allow linear deformation with minimal resistance. A dilatometer (Figure 3.6) is used to periodically measure specimen length, starting from the time of final set.

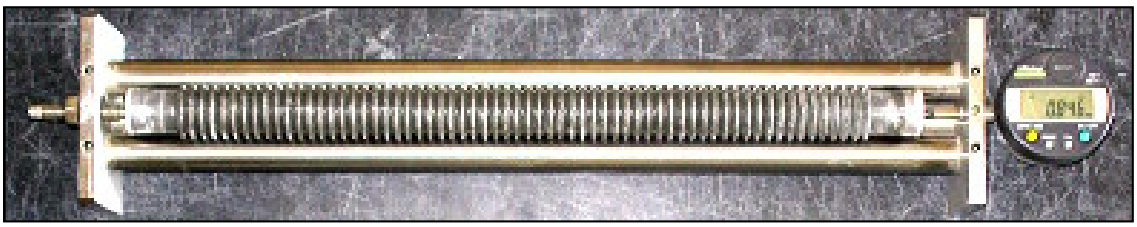

Figure 3.6. Autogenous shrinkage specimen in dilatometer measurement device.

Autogenous shrinkage was measured in 86 cement paste specimens with varying $LiNO_3$ dosages. Triplicate paste specimens at each of the $LiNO_3$ dosages of 0%, 50%, 100%, 200%, and 400% were measured for Cement 6, both with and without 20% fly ash replacement. Triplicate specimens at each of the $LiNO_3$ dosages of 0%, 100%, and 400% were tested for the remainder of the cements in Table 3.1.

Prior to mixing, cement, fly ash, lithium nitrate solution, and de-ionized water were stored at 25 degrees Celsius and 50% relative humidity in environmental chambers for 48 hours to minimize initial differences between paste specimens.

The procedure for mixing of each paste followed ASTM C 305-99, Standard Practice for Mechanical Mixing of Hydraulic Cement Pastes and Mortars of Plastic Consistency, with two modifications. First, the lithium nitrate solution was stirred into the water in the mixing bowl before the cement was added. Secondly, mixing was paused twice during the prescribed 90 seconds for scraping paste down from the sides of the bowl, rather than once, as ASTM C 305 instructs.

After mixing, the paste was pressed by hand into plastic corrugated tubes. Tapping the specimen ends on the countertop was necessary to facilitate paste flow into the tubes. The ends were capped with hard plastic caps, and sealed with Para-film. After the specimens were prepared, they were placed in environmental chambers, on corrugated plastic sheets which held them in straight lines as the paste hardened.

Autogenous shrinkage specimens were made from the same mixing batches as the Vicat time of setting specimens. Initial autogenous shrinkage specimen length measurements were taken when the Vicat specimens reached final set. After the initial reading and between all subsequent readings, the specimens were kept in the

environmental chambers. For the duration of the project, temperatures in these chambers were observed to fluctuate within a range of 24.5±0.4 degrees Celsius, and relative humidity was observed to fluctuate between 47 and 51%.

Two significant deviations from Jensen and Hansen's procedure were the use of an environmental chamber to control the temperature of the specimens rather than a glycol bath, and the periodic manual measurement of specimen length, rather than the use of an automatic data logger.

3.2.7 Free Shrinkage

Linear deformation due to unrestrained shrinkage (combined autogenous and drying shrinkage) was measured in concrete prisms by ASTM C 157-04, Standard Test Method for Length Change of Hardened Hydraulic-Cement Mortar and Concrete. Unlike the chemical and autogenous shrinkage tests, free shrinkage testing included effects of drying shrinkage and the restraining effects of aggregates. Effects of lithium nitrate on free shrinkage were examined using Cement 6, both alone and with 20% replacement by Class F fly ash. Lithium was dosed at 0%, 50%, 100%, 200%, and 400% for both of these cases.

A water-to-cement ratio of 0.30 was used in mixing the concrete for these specimens. Coarse and fine aggregate was used at the same proportions as full scale batches used at the Hartsfield-Jackson Atlanta International Airport, shown in Table 3.4. The #4 coarse aggregate, however, was too large for use in the free shrinkage molds. The #67 aggregate was therefore used for the entire coarse aggregate amount. The steel molds used to make the prismatic specimens were 3 in x 3 in x 11 ¼ in, with gage studs

at each end. Mixing procedure was consistent with ASTM C 192-05, Standard Practice for Making and Curing Concrete Test Specimens in the Laboratory, except that the number of rodding strokes to consolidate the concrete in the molds was increased from 34 to 50 strokes per layer after early batches failed to consolidate sufficiently due to the low flowability.

After mixing and molding the concrete specimens, the specimens were covered in wet burlap and kept in a temperature-controlled environment for 24 hours, then de-molded, measured, and kept in environmental chambers set at 25 degrees Celsius and 50% relative humidity. Specimens were stored at least one inch from each other and all other surfaces in the environmental chambers, and on steel racks, as shown in Figure 3.7, to allow air flow and moisture transfer from all sides of the specimens. Subsequent length measurements allowed for shrinkage calculation.

Figure 3.7. Free shrinkage specimens in environmental chamber storage.

A significant deviation from ASTM C 157-04 is that the specimens were not cured for 28 days in lime saturated water before measurements began. Of particular interest in this research was the combined effect of autogenous and drying shrinkage on the concrete specimens. For drying and autogenous shrinkage to occur simultaneously, as in field conditions, measurements were required to be taken during the first 28 days, and specimens were required to be in an environment that allowed drying shrinkage.

3.2.8 Restrained Shrinkage

Effects of lithium nitrate addition on the age at cracking of restrained concrete was investigated using restrained rings as described in ASTM C 1581-04, Standard Test Method for Determining Age at Cracking and Induced Tensile Stress Characteristics of Mortar and Concrete under Restrained Shrinkage. Effects of $LiNO_3$ dosages of 0%, 50%, 100%, 200%, and 400% were tested in concrete specimens made from Cement 6, both alone and with 20% replacement by Class F fly ash. One specimen for each case was tested, for a total of 10 rings.

A water-to-cement ratio of 0.30 was used in mixing the concrete for these specimens. Coarse and fine aggregate was used at the same proportions as full scale batches currently in production at the Hartsfield-Jackson Atlanta International Airport shown in Table 3.4. The #67 aggregate was substituted for the #4 aggregate used in the field batches, however, because the #4 was too large according to ASTM C 1581-04. Mixing procedure was consistent with ASTM C 192-05, Standard Practice for Making and Curing Concrete Test Specimens in the Laboratory.

Molds similar to those described in ASTM C 1581 were used, each consisting of a steel ring mounted to a flat steel plate, around which the concrete was cast. An outer ring

of stiff cardboard, cut from a concrete-forming construction tube and wrapped in plastic to prevent water absorption, was used to form the outer surface of the specimen ring.

After being molded, the concrete specimens were covered in wet burlap and placed in a temperature and moisture-controlled room. After 24 hours, the outer rings were removed from the specimens, and the top surface was coated with paraffin wax to limit drying to the outer side edges of the specimen, as ASTM 1581 describes. Specimens were kept in the temperature and moisture-controlled room for the next 28 days with shrinkage restrained by the inner steel ring. ASTM C 1581-04 describes the use of a data acquisition system with strain gages mounted to the steel ring of each specimen to determine the exact time of cracking. In this research, the rings were visually checked daily for cracks, rather than using a data acquisition system.

Figure 3.8. Restrained shrinkage setup.

3.2.9 Strength

Effects of lithium nitrate on the strength of concrete specimens were investigated both at Georgia Tech and by an outside consultant, as partners in the Innovative Pavement Research Foundation Project number FAA-01-G-002-04-6.

Effects of lithium nitrate addition on the compressive strength of concrete were investigated at Georgia Tech, using $LiNO_3$ dosages of 0%, 50%, 100%, 200%, and 400%. For each of these dosages, five 4-inch by 8-inch concrete cylinders were made using Cement 6, with 20% Class F fly ash replacement. A water-to-cement ratio of 0.30 was used in mixing the concrete for these specimens. Coarse and fine aggregate and admixtures were used at the same proportions as full scale batches currently in production at the Hartsfield-Jackson Atlanta International Airport shown in Table 3.4. The #67 aggregate was substituted for the #4 aggregate, however, because the #4 aggregates were too large for the cylinder molds. Mixing procedure was consistent with ASTM C 192-05, Standard Practice for Making and Curing Concrete Test Specimens in the Laboratory. Specimens were capped and stored at room temperature for 24 hours, de-molded, and then placed in a high humidity fog room. Before being tested, the cylinders were ground flat on the ends using a handheld electric grinder. Compression testing of these cylinders was performed at 28 days, and was consistent with ASTM C 39-05, Standard Test Method for Compressive Strength of Cylindrical Concrete Specimens.

Flexural and compression test specimens were produced in the field from full scale production batches at Hartsfield-Jackson Atlanta International Airport, using lithium nitrate dosages of 0%, 50%, 100%, 200%, and 400%. These flexural and

compression test specimens (Figures 3.9 and 3.10) were tested at 36 hours, 48 hours, 72 hours, 7 days and 28 days, and were consistent with ASTM C 39-05, Standard Test Method for Compressive Strength of Cylindrical Concrete Specimens, and ASTM C 78, Standard Test Method for Flexural Strength of Concrete (Using Simple Beam with Third-Point Loading). The Cement 6 used in these batches was from a different batch than the cement used for laboratory tests, with slightly different oxide composition. Oxide analysis of the two batches of Cement 6 used in Georgia Tech lab testing and in the consultant's production batch strength testing are compared in the Appendix.

Figure 3.9. Compression test cylinders from field mix at Hartsfield-Jackson Atlanta International Airport

Figure 3.10. Compression test cylinders from field mix at Hartsfield-Jackson Atlanta International Airport

CHAPTER IV

Results and Discussion

In this chapter, results from isothermal calorimetry, rheology and bleed water testing, time of setting, chemical shrinkage, autogenous shrinkage, free and restrained concrete shrinkage, and compressive and flexural strength testing are presented and compared to any existing findings in the literature.

4.1 Isothermal Calorimetry

Isothermal calorimetry was performed at 25°C on cement pastes from all cements, as well as Cement 6 with 20% Class F fly ash replacement, at 0%, 50%, 100%, 200% and 400% dosages.

In general, as the dosage of lithium nitrate increased, early heat of hydration increased, and the early hydration reactions (i.e., hydration of C_3S and C_3A) were generally accelerated. This is apparent by in the heat of hydration curves in Figures 4.1 through 4.7. At higher admixture dosages, the curves shift upward and the peaks shift to the left. Also, the second "hump" of the heat profile appears to shift to the left slightly more than the overall profile. This second hump is generally attributed to reactions of the C_3A component of the cement.

Figures 4.1 through 4.3 illustrate the heat of hydration effects of lithium nitrate on Cements 1, 2, and 3, (the low, moderate, and high alkali cements, with compositions given in Table 3.1). Figure 4.1 illustrates earlier heat generation for each increase in lithium nitrate dosage. However, data for the moderate and high alkali Cements 2 and 3, in Figures 4.2 and 4.3, suggest that above some level of lithium dosage, further increases

in heat of hydration do not occur. In the high alkali Cement 3 in Figure 4.3, the 50% dosage appears to increase the early heat of reaction, but no further increases are apparent above the 50% lithium dosage (corresponding to 1.5 gallons per cubic yard for the admixture and mix design in Table 3.4). In the moderate alkali Cement 2 in Figure 4.10, no further increases are apparent above 200% dosage (corresponding to 3.4 gallons per cubic yard.) The low alkali Cement 1 shows continued heat increases up to the highest level tested, 400% dosage (corresponding to 4 gallons per cubic yard.) Apparently, low alkali cements continue to generate greater early heat at increasing lithium dosages, while higher alkali cements reach a maximum heat of hydration profile at lower dosages. These results suggest that lower alkali cements are more susceptible to greater heat evolution increases due to the addition of the lithium admixture .

Bentz (2005) also observed acceleratory effects of lithium admixture, and concluded that they are similar to the acceleratory effects of potassium and sodium ions (all three are Group I alkali elements, with 1 valence shell electron). Potassium and sodium ions, which may be introduced into the mix water from the cement or added as soluble salts to the mix water, reduce the solubility of calcium ions, promoting nucleation of calcium-containing hydration products (Jawed,1978). Since the acceleratory period of the hydration of tricalcium silicate (C_3S) is likely governed by this nucleation (Odler, 1979), increases in the alkai concentration in solution accelerate the hydration of C_3S. Results in Figures 4.1 through 4.3, which show acceleration at increasing dosages of $LiNO_3$, suggest that in these systems lithium ions may have similar effects on the solubility of calcium ions in solution, on the nucleation of calcium-containing hydration products, and on cement hydration acceleration.

The upper limit on the acceleratory effects of increasing dosages of lithium nitrate shown in Figures 4.2 and 4.3 suggests that above some lithium ion concentration, increases in lithium concentration have diminishing effects on nucleation of hydration products. Since this upper limit or "threshold" may be reached at a lower lithium dosage in the high alkali cement, it is likely that nucleation is affected by the combined alkali ion concentration: $[Li^+ + Na^+ + K^+]$. At some level of total alkali ion concentration, a maximum early heat generation profile is reached. It is proposed that this alkali ion concentration is reached at lower lithium dosages for high alkali cements, because the total alkali concentration is already very high due to the contribution of the cement alkalis.

Of significance in this observation is that the cements which are most vulnerable to hydration acceleration are also the cements that are most likely to be combined with lithium admixture in practice. Low alkali cements are typically specified in applications where ASR is a consideration, and appear to be accelerated more by $LiNO_3$.

Figures 4.4 through 4.6 illustrate the heat of hydration effects of lithium nitrate on Cements 4, 2, and 5, respectively (the low, moderate, and high C_3A cements whose compositions are given in Table 3.1). All three cements show increased early heat generation with the addition of lithium nitrate. The data in Figure 4.4 for the low C_3A Cement 4 show an acute shift to the left, indicating a significantly faster rate of reaction with increasing addition of lithium. Figure 4.5 illustrates a similar shift to the left for the moderate C_3A Cement 2. The data for the high C_3A Cement 5 in Figure 4.6, however, show only a very subtle shift to the left at increasing dosages. This suggests that the accelerating effects of lithium nitrate on the hydration reactions are less noticeable in

higher C_3A cements. This may be due to the higher sulfate levels present in high C_3A cements. Also, the high C_3A cement had slightly higher alkali content than the other cements in this comparison, and this may have limited its acceleration.

In addition to the aforementioned acceleration of the C_3S reactions by effects of lithium ions on nucleation, there appears to be an acceleration of the C_3A reactions as well. This acceleration, most apparent in the moderate alkali / moderate C3A Cement 2 in Figures 4.2 and 4.5, is indicated by a change in the overall shape of the heat generation profile. The Control mix (0% Lithium) curve in Figure 4.2 shows a 4 to 6 hour delay between the main (C_3S) peak and the secondary (C_3A) peak. The 50% lithium nitrate dosage curve for the same cement, however, shows only an approximate 2 hour delay. At progressively higher lithium nitrate dosages, the C_3A peak shifts left relative to the C_3S peak, so that at the 400% dosage, the two peaks are nearly aligned. This behavior is also clearly visible in the Cement 1 curves in Figure 4.1, but is less evident in the other cements. This behavior may be related to effects of lithium on the rate of C_3A dissolution. Alkalis (sodium and potassium) have been shown to promote the dissolution of C_3A, accelerating subsequent reactions (Jawed, 1978). Alkalis often, in fact, serve as rapid set accelerators for quick or flash-setting concretes and spray-dried shotcrete (Hewlett, 1998). Figures 4.1 and 4.2 suggest that lithium, also a Group I alkali, may similarly promote C_3A dissolution, and accelerate C_3A hydration.

Gypsum ($CaSO_4 \cdot 2H_2O$) is typically added to cement to reduce the rate of dissolution of C_3A and to delay its very rapid hydration. If adequate gypsum is not present, the C_3A reactions are accelerated, and in extreme cases the formation of aluminate hydrate may cause flash-setting. If too much gypsum is present, excessive

ettringite formation may cause premature stiffening of the fresh concrete. An optimal amount of gypsum avoids these two extremes, retards the C_3A reactions, and produces concrete with high 28-day strength and low shrinkage. This optimal amount of gypsum is a function of the C_3A content, the alkali content, and the fineness of a cement (Jawed, 1978). The C_3A reaction acceleration that lithium nitrate appears to cause, particularly in Figures 4.1 and 4.2, is significant because it affects this optimal retardation of the C_3A reactions by gypsum. If unchecked, some negative effects on workability, time of setting, shrinkage, and strength may be apparent, depending upon the lithium admixture dosage, and relative C_3A and gypsum contents of the cement.

In addition to the examination of the cements of varying composition described above, isothermal calorimetry was also performed on Cement 6 alone and with Class F fly ash replacement at 20% by weight of cement (Figures 4.7 and 4.8); again, oxide analyses for these materials are given in Table 3.1. As expected, at a constant w/cm of 0.30, lower heats were generated with the 20% fly ash replacement than with the cement alone, due to the dilution of the cement by the use of fly ash. In these plots, heat generated is reported as joules per gram of cementitious material, including the fly ash.

For Cement 6 paste without fly ash, the addition of lithium nitrate produced both higher early heat generation and acceleration of early hydration reactions, consistent with observed behavior in Figures 4.1 through 4.6. However, in the 20% fly ash case in Figure 4.8, both of these effects are less severe. Figure 4.9 compares the heat of hydration increases due to 400% lithium dosage (over the control) in the Cement 6 alone and Cement 6 with fly ash mixes. Effects on heat of hydration are clearly less significant with the Class F fly ash. This suggests that Class F fly ash replacement may decrease the

(possibly negative) effects of lithium nitrate on early heat of hydration. This is significant because Class F fly ash, due to its ASR-mitigating effects, is likely to be used in lithium-containing mixes.

The reduced lithium effects on early heat of hydration in Class F fly ash mixes may be partially due to lithium binding in the calcium silicate hydrate (C-S-H) structure. As discussed in Section 2.3, the reduced calcium-to-silica ratio of a Class F fly ash mix increases lithium binding in the C-S-H structure. Since more of the lithium is bound in the C-S-H structure, less free lithium is present in the mix water and subsequent pore solution, so it is not unexpected that effects of lithium will be diminished in these mixes.

There is some concern that this increased binding of lithium will decrease the effectiveness of lithium nitrate admixtures at ASR mitigation. However, regardless of the reduced free lithium available to suppress ASR, combinations of lithium nitrate and Class F fly ash have shown synergistic effects. Use of both provides better ASR mitigation than either alone. So while calorimetry does indicate that more lithium may be bound in the C-S-H structure if Class F fly ash is present, Class F fly ash is still beneficial, as it increases ASR durability and diminishes potentially adverse heat of hydration effects of the lithium.

Figure 4.10 shows longer-duration calorimetry results for Cement 6, including cumulative heat evolution data to 96 hours of age. For both the cement alone, and with the 20% fly ash replacement, cumulative heat curves for the control (no lithium) case exceed that for the 400% dosage case after 1 day. Although the lithium-dosed pastes generate more heat initially, cumulative heat after one day is lower than that for the control (no lithium) mix. At two and three days, cumulative heat for the control mixes is

6 to 10% higher than for the 400% mixes. Similar behavior was observed in several of the other cements. This may indicate a lower degree of hydration is achieved at a given time, and that the initial rapid hydration and presumed associated product formation may result in a subsequent retarded rate of hydration. It also may indicate, however, that the different C-S-H structure that forms in the presence of lithium ions, due to different bond energies, simply releases less heat. Because the data here was collected only to 96 hours of age, it is not clear if the cumulative heat of hydration in the lithium-containing pastes will continue to be suppressed. Cumulative heat curves for the other cements in this research are shown in Appendix A. Further research, including longer term isothermal calorimetry data, is necessary to better understand these observations and their relationship to cement composition, strength gain, and durability.

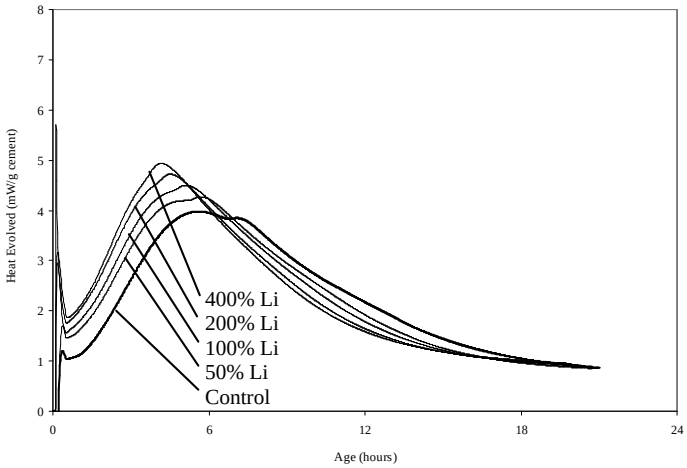

Figure 4.1. Calorimetry results for Cement 1 (Low Alkali).

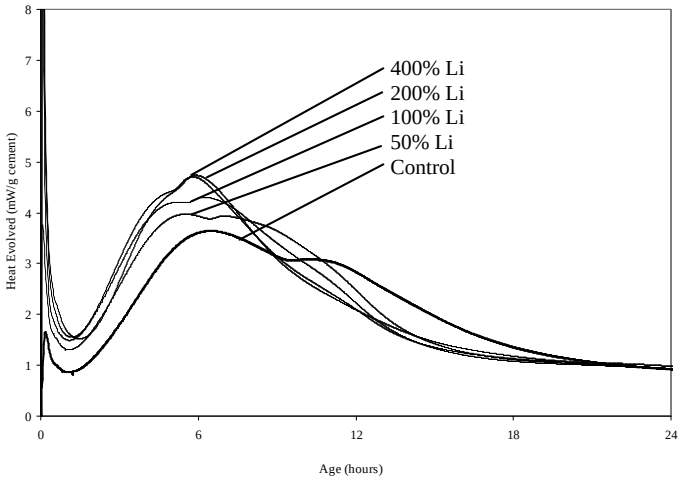

Figure 4.2. Calorimetry results for Cement 2 (Moderate Alkali).

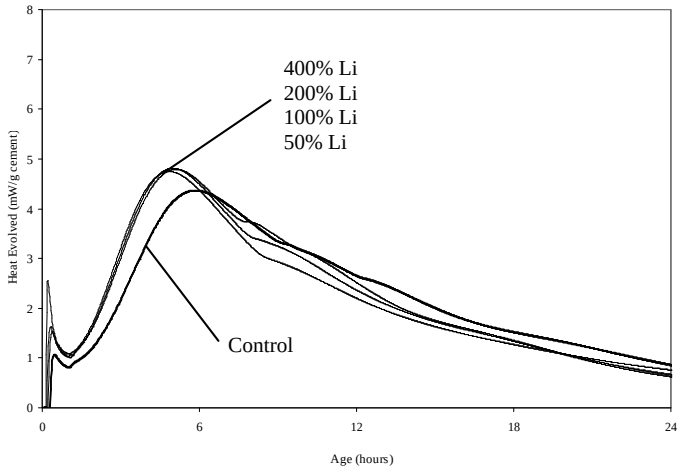

Figure 4.3. Calorimetry results for Cement 3 (High Alkali).

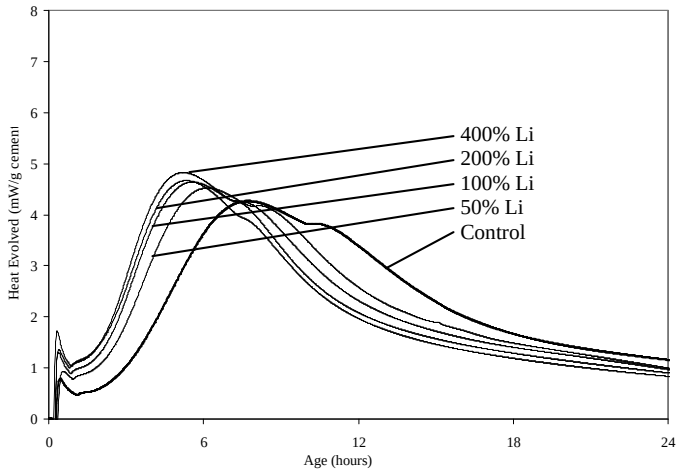

Figure 4.4. Calorimetry results for Cement 4 (Low C_3A).

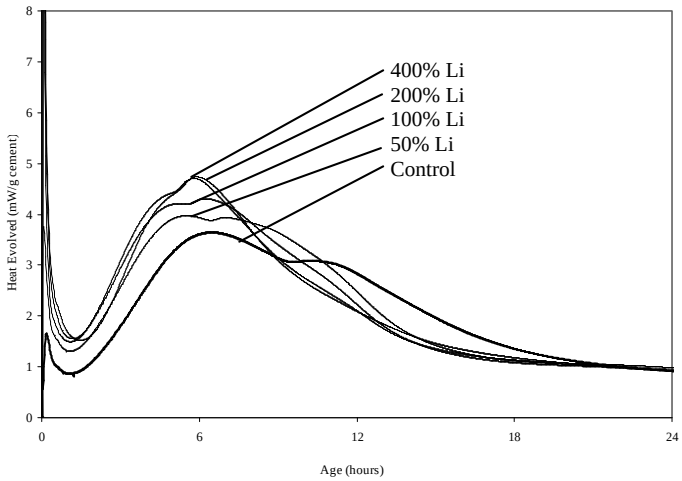

Figure 4.5. Calorimetry results for Cement 2 (Moderate C_3A).

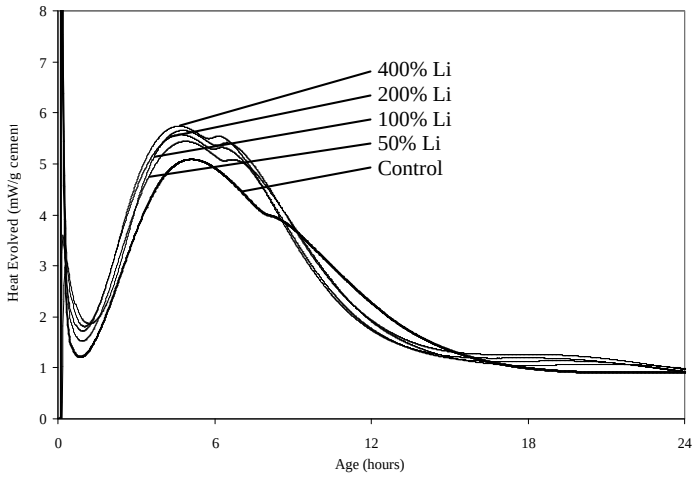

Figure 4.6. Calorimetry results for Cement 5 (High C_3A).

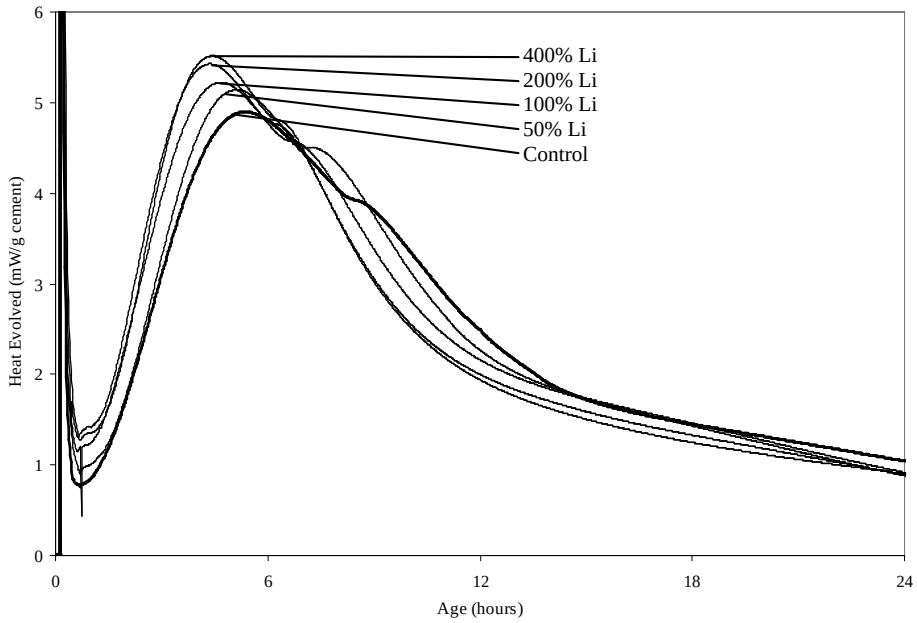

Figure 4.7. Calorimetry results for Cement 6 with no Class F fly ash.

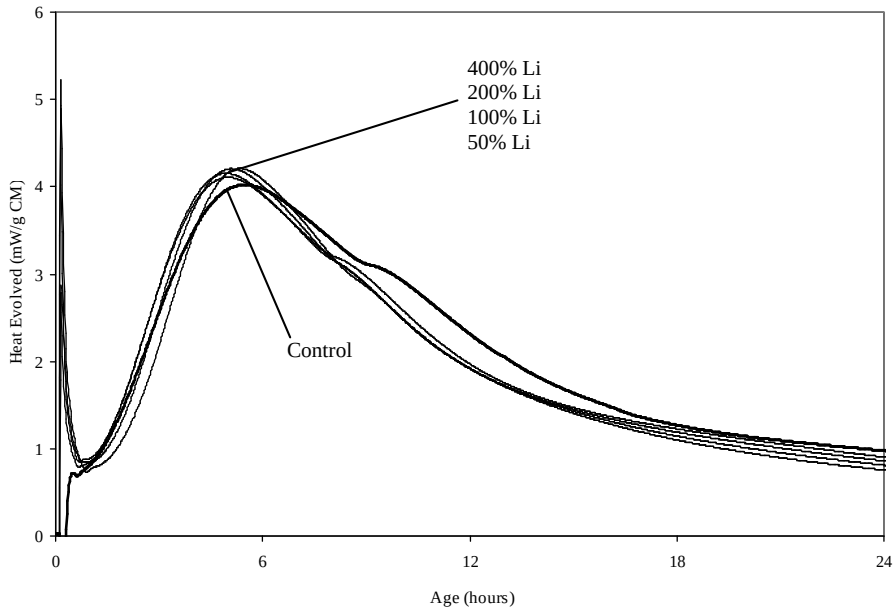

Figure 4.8. Calorimetry results for Cement 6 with 20% Class F fly ash replacement.

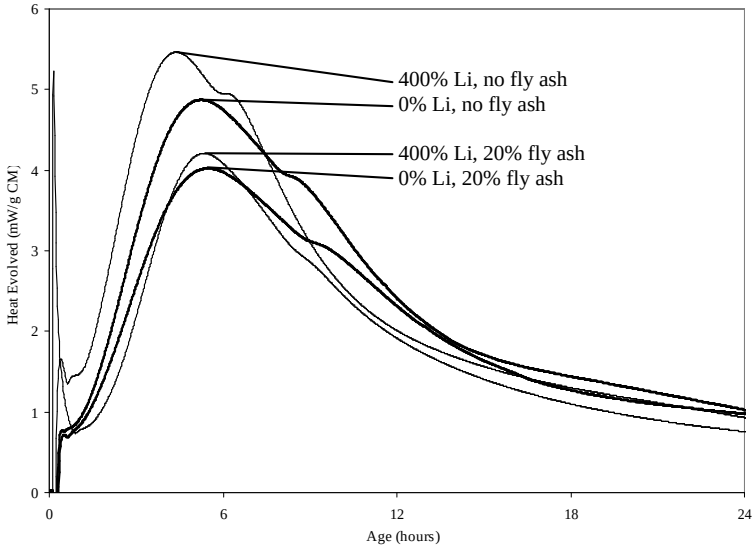

Figure 4.9. Cement 6 alone and with 20% fly ash replacement.

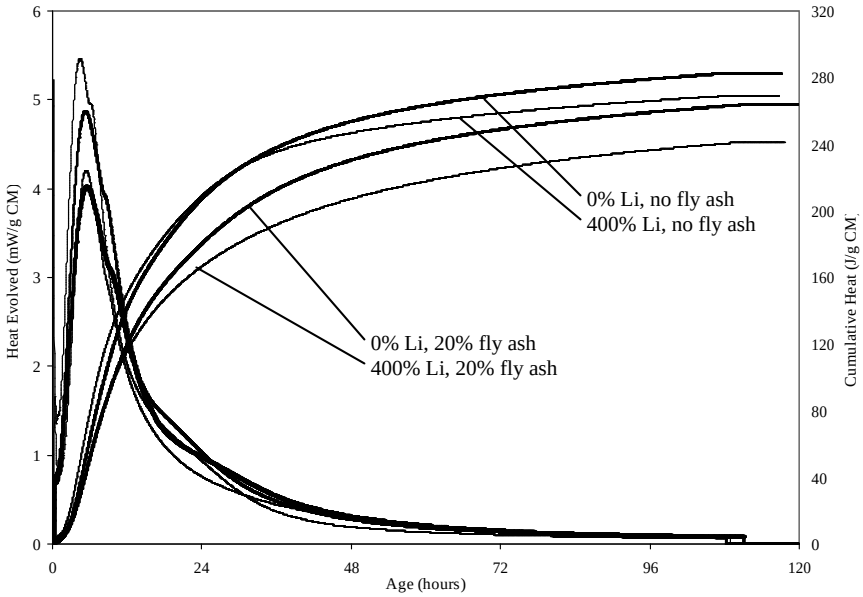

Figure 4.10. Cement 6 cumulative heat.

4.2 Workability

A typical airfield pavement mix design was tested for lithium nitrate effects on bleed water (ASTM C 232-04 Standard Test Method for Bleeding of Concrete) and slump (ASTM C 143-05 Standard Test Method for Slump of Hydraulic-Cement Concrete), at lithium nitrate dosages up to 400% of the standard dosage. No measurable bleed water was observed for any of the mixes, likely due to the low w/cm used (0.30). All slump measurements, for mixes with lithium nitrate dosages up to 400%, were less than ¼ inch, with no detectable influence of $LiNO_3$.

Further workability testing was performed on concrete mixes using a higher w/c of 0.45. Mix proportions for these batches are shown in Table 3.5 of Chapter 3 of this report. Effects of lithium nitrate dosages of 0%, 100%, and 400% were investigated. Slump and rheometer testing was performed on these concrete batches. Concrete is assumed here to behave as an ideal Bingham fluid, with flow behavior characterized by:

$$\tau = \tau_0 + \eta \, d\gamma/dt$$

where τ = shear stress, τ_0 = yield stress, η = plastic viscosity, and $d\gamma/dt$ = shear rate.

Measurements of torque and speed at two probes on the rheometer provided data representing the viscoplastic behavior of these concrete mixes. Assuming ideal Bingham material behavior, lines that fit to these data provide relative yield stress and relative viscosity parameters expressed in terms of torque and speed. Reported values of these parameters in Tables 4.1 and 4.2 were taken as the averages of three values taken from

three sets of rheometer data readings for each mixture. Standard deviation values in Tables 4.1 and 4.2 represent variations between the parameters calculated from the three data sets, but are not representative of the data scatter within each data set. The average values for these parameters are illustrated graphically in Figure 4.11, with the relative yield stress idealized as a yield point, and the relative viscosity represented by the slope of the plastic regions of the curves. Table 4.1 also includes slump values from one measurement per mix.

Relative Bingham yield stress values for the control mix and the 100% lithium nitrate dosage mix in Table 4.1 show no significant difference, suggesting that the standard dosage of admixture has little effect on this parameter. The 400% dosage mix, however, shows a 28% decrease in yield stress, suggesting that larger-than-typical dosages of admixture may alter workability. Slump values, largely dependent on the yield stress parameter, confirm this lithium nitrate effect on yield stress behavior.

No clear trend with lithium admixture dosage is evident in the relative viscosity values in Table 4.2. The relative viscosity appears to decrease by 8 % in the 100% dosage mix, but increase by 83 % in the 400% dosage mix, as compared with the control.

Figure 4.11 illustrates the ideal Bingham material behavior characterized by these parameters. A Bingham material behaves as a solid at stresses below a yield stress, and flows as a viscous liquid above that yield stress. Figure 4.11 shows little difference between the behavior of the control mix and the 100% mix, but effects of the 400% dosage appears significant in this figure. Thomas et al.(2003) found similar results for the standard dosage in mixes with w/cm of 0.35, in that the standard dosage had little effect on slump, but higher dosages were not tested.

Standard deviations within each mix are small compared to the differences between the Control and 400% dosage parameters. However, the standard deviation values do not account for variance in the data used to calculate the parameters used to obtain these averages. Average values came from three calculated parameters, from three separate sets of data, for each mix. R-values were low for all of these data sets, ranging from 0.01 to 0.25 (1.0 representing perfect correlation). The scatter of data points used to obtain parameters is illustrated in Figure 4.12, showing data points from all three measurements of the control mix.

Behavioral differences between the control mix and the 400% dosage mix are not clear in Figure 4.13, where all data from the three measurements from each of these two mixes has been presented together. Data obtained below speeds of 0.05 m/s appear similar for both mixes, but there is a shortage of 400% dosage mix data above 0.10 m/s. Since both of these mixes behaved similarly at speeds of 0.07m/s, and the 400% dosage mix appears to have a lower Bingham yield stress, it was expected that the slope of the 400% dosage mix line should be steeper (higher viscosity) below 0.07 m/s. However, if the Bingham linear representation is not a true representation of behavior of the fresh concrete, and since the 400% data points are lacking above 10 m/s, it is unclear if the 83% increase in viscosity is accurate at higher speeds. In retrospect, the slopes of the lines (representing the plastic viscosity) may have been more accurately defined if the rheometer had been operated at higher speeds in some of the tests.

Although the Bingham equation, utilizing a linear fit to flow data, is most commonly used to characterize concrete flow behavior, nonlinear models have been shown to more accurately represent concrete in some cases. The Herschel and Buckley

equation and the Power equation both use an exponent on the shear rate term to account for nonlinearity in concrete's flow behavior. A Power equation fit to the Control mix and 400% dosage mix data is shown in Figure 4.14. The slope (viscosity) of the 400% mix does appear to decrease at higher speeds, and R-squared values are slightly better than with the linear Bingham idealization, but conclusions are similar. The 400% dosage mix appears to have a lower yield stress, and more viscous flow above that yield stress, than the Control mix.

Although the data scatter yields the rheometer-obtained parameters somewhat questionable, there is agreement between trends in yield stress in both the Bingham model and the Power equation model, as well as the slump measurements. The 1.25 inch increase in slump of the 400% dosage mix over the control is roughly 3 times the single-operator standard deviation stated in the precision section of ASTM C 143 for slumps of 6.5 inches (none is listed for slumps closer to 8.5 inches). Overall, it does appear that the Bingham yield stress of concrete is decreased at the 400% dosage rate, and therefore slump is increased. Data also suggest that the use of lithium nitrate may affect concrete plastic viscosity, but further testing is necessary to confirm this.

Table 4.1 Relative Bingham yield stress parameters from rheometer vs slump testing

	Rheometer Yield-stress (N mm)		Slump
	Average	Std Dev	(in)
Control Mix	977	75	8
100% LiNO3 Mix	971	40	8.5
400% LiNO3 Mix	704	179	9.25

Table 4.2 Relative viscosity (N mm sec / m)

	Average	Std Dev
Control Mix	5404	1264
100% LiNO3 Mix	4976	1126
400% LiNO3 Mix	9897	1659

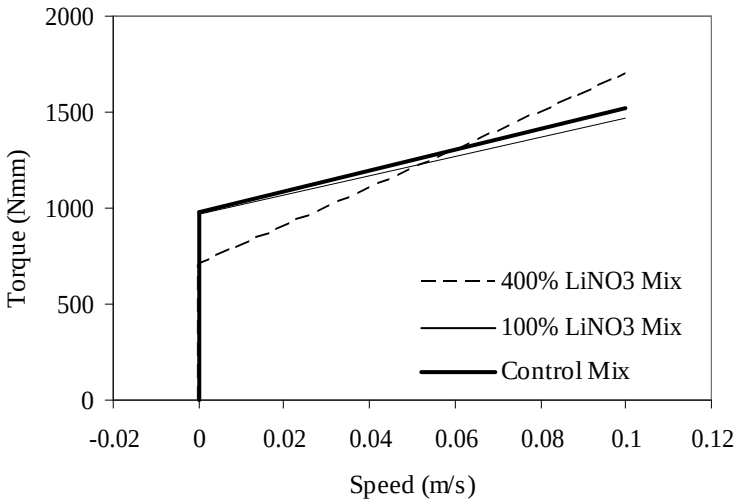

Figure 4.11 Viscoplastic idealizations of the behavior of concrete mixes dosed with lithium nitrate.

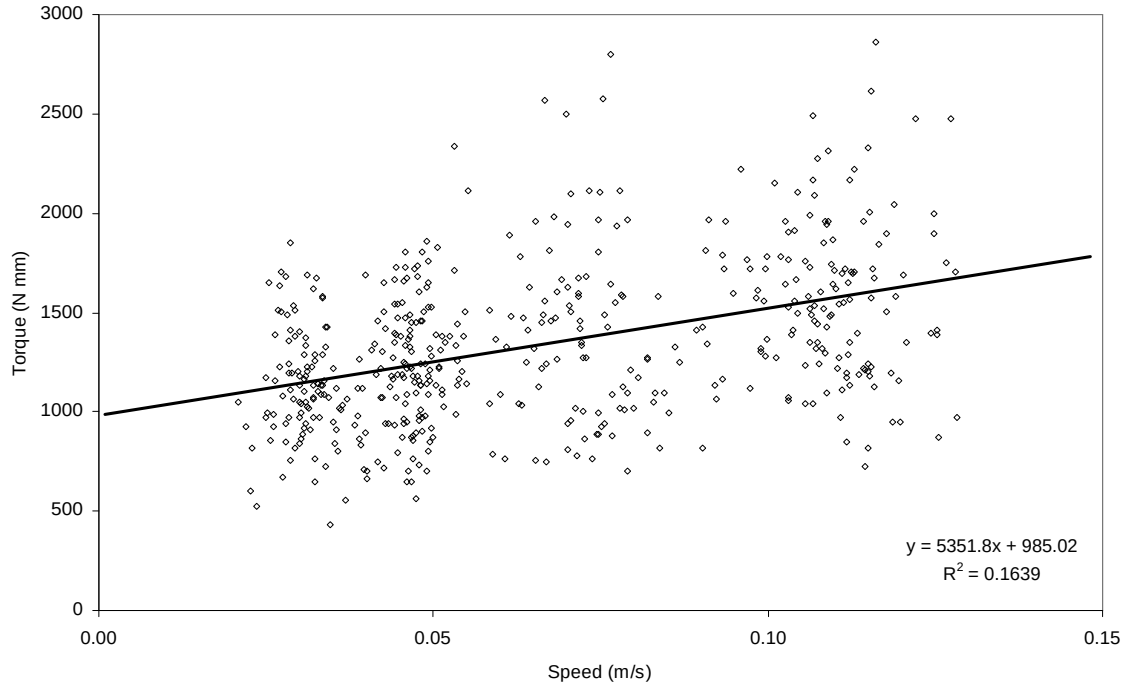

Figure 4.12 Rheology data for the Control mix, with linear least-squares trend line fit to data.

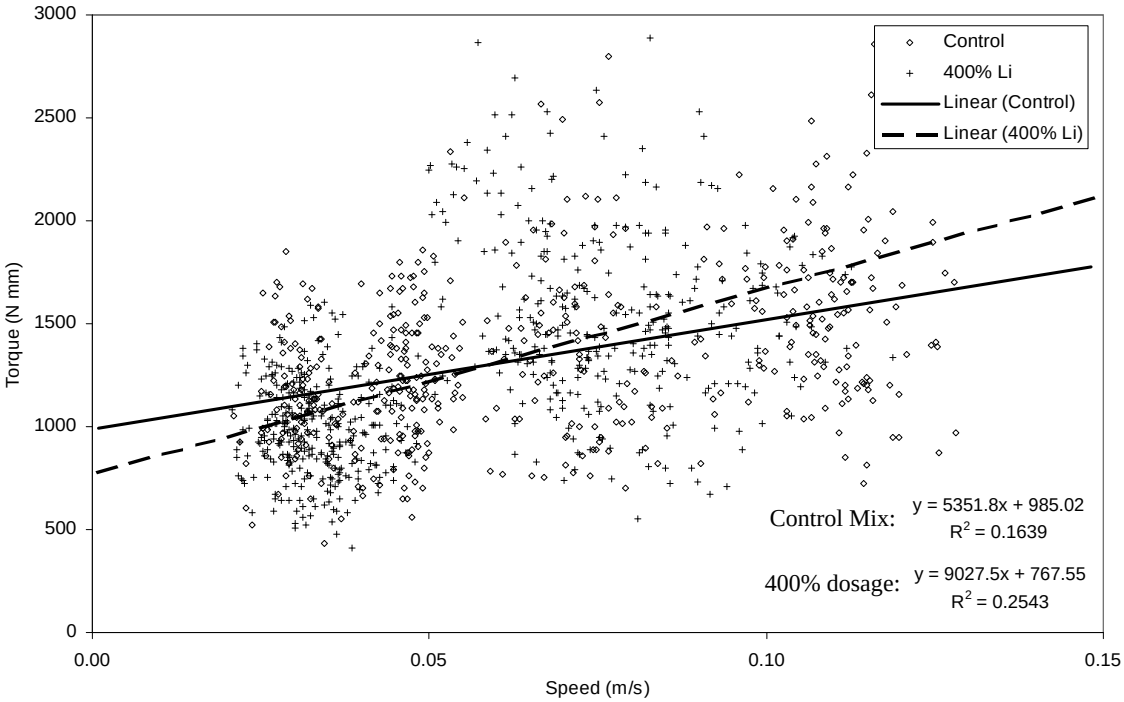

Figure 4.13 Combined rheology data for Control and 400% dosage mixes, with linear trend lines fit to data.

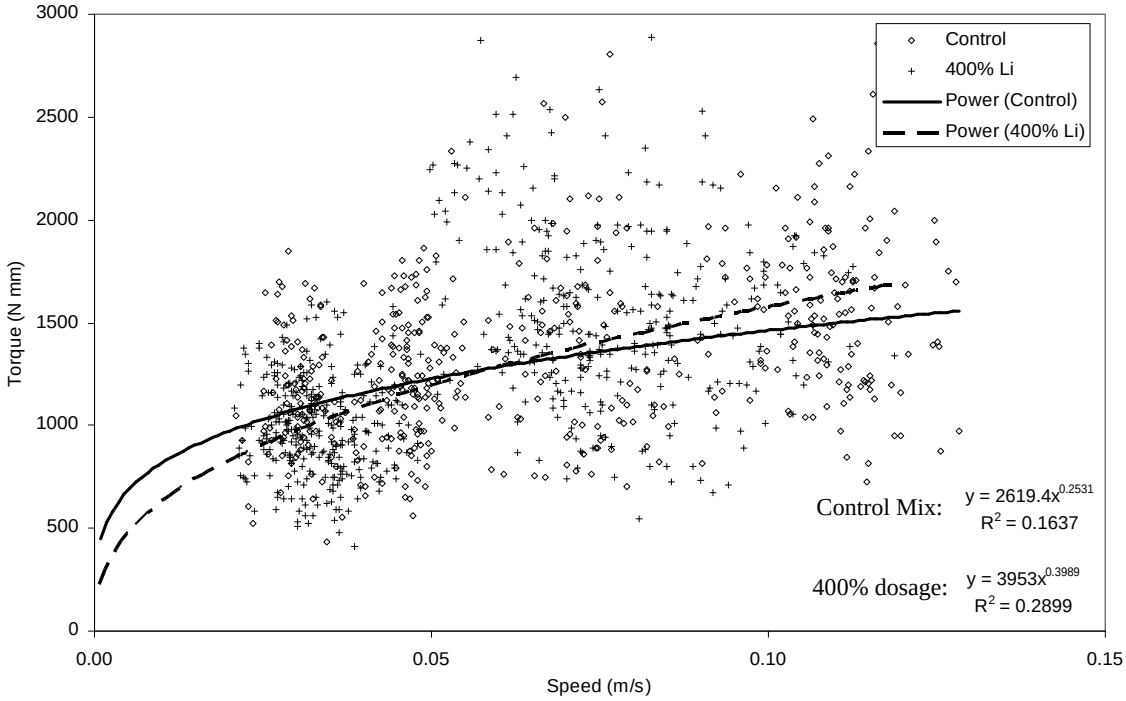

Figure 4.14 Combined rheology data for Control and 400% dosage mixes, with power function fit to data.

4.3 Setting Time

Effects of lithium nitrate on setting times of cement paste specimens were investigated by ASTM C 191-04 Standard Test Methods for Time of Setting of Hydraulic Cement by Vicat Needle. Pastes were prepared at w/cm of 0.30. Cements at 3 alkali levels, 3 C_3A levels, plus Cement 6 alone and with 20% fly ash replacement were tested. Of the seven cement cases tested, the only cement to show a setting time dependency on lithium dosage was the low alkali Cement 1, with a Na_2O_e of 0.295%. In the Cement 1 tests, the standard dosage of lithium nitrate decreased the initial setting time by 15%, and the final setting time by 22%. Figure 4.15 shows results from Vicat testing with this cement. Figures 4.16 through 4.21 show Vicat test results for the other cements tested.

As expected, Figures 4.16 and 4.17 indicate that higher setting times were observed with the use of fly ash. However, no clear effect of lithium nitrate was observed in Cement 6 with or without fly ash replacement.

It may be significant that the only cement to be affected by the lithium nitrate admixture is the lowest alkali cement, and that calorimetry testing suggests that lower alkali cements are more susceptible to hydration reaction acceleration. The lithium sensitivity of a cement likely depends on more variables than just alkali content, but alkali content is likely a factor.

Of further significance in these results is that although calorimetry showed acceleration of the C_3A reactions to some extent in all cements, the negative behaviors associated with C_3A acceleration were not observed in time of setting tests at lithium dosages up to 400%. There were no indications of early stiffening or flash-set at any dosage, and the reduction in set time for the low alkali cement is likely not of the magnitude to impair construction operations in the field.

In order to more accurately simulate actual conditions in the field, additional Vicat time of setting tests were performed at an elevated temperature of 35 degrees Celcius, using Cement 6 with and without fly ash. As expected, fly ash replacement increased initial and final setting times. However, no $LiNO_3$ effects were apparent at any dosage. Results for these elevated temperature Vicat tests are shown in Appendix B.

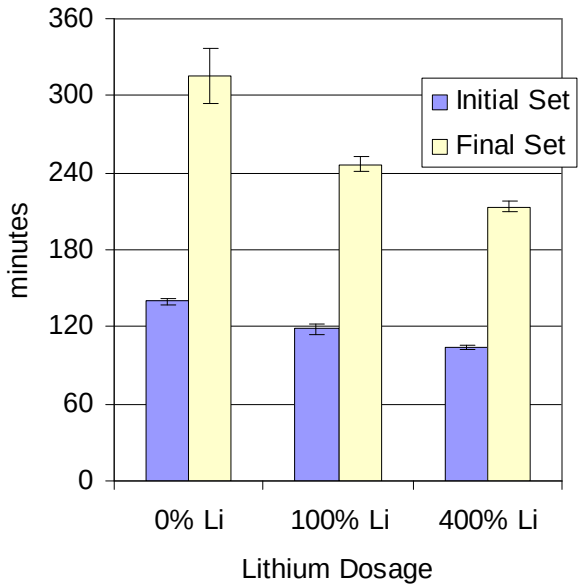

Figure 4.15. Vicat setting times for Cement 1 (low alkali).

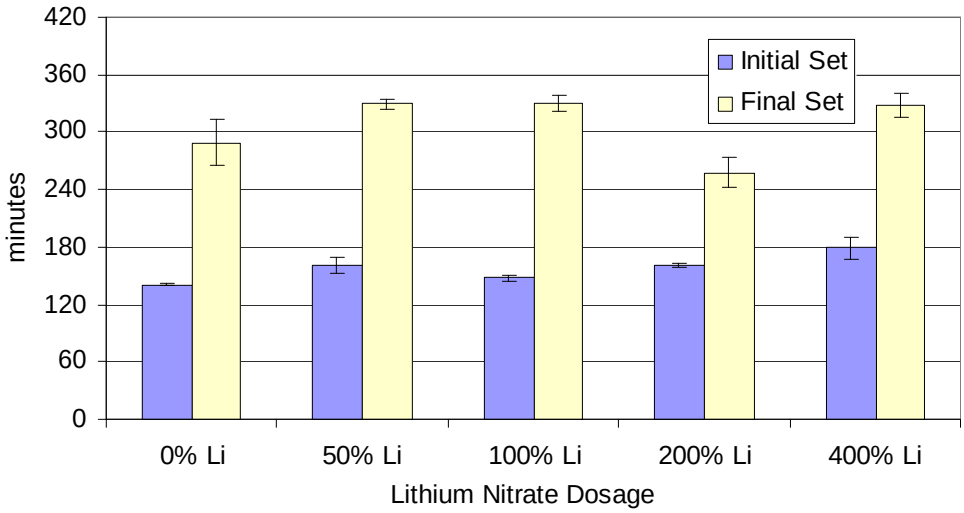

Figure 4-16. Vicat setting times for Cement 6 with 20% fly ash replacement.

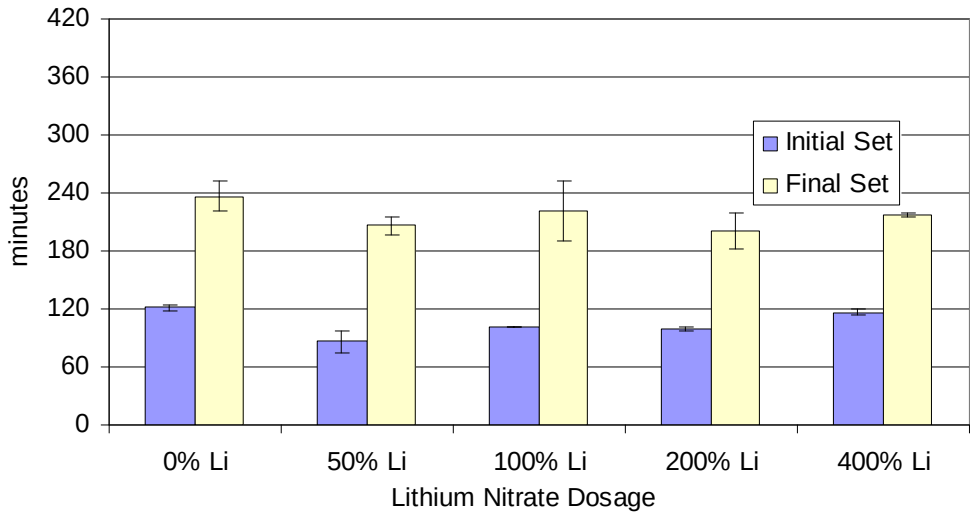

Figure 4.17. Vicat setting times for Cement 6, with no fly ash.

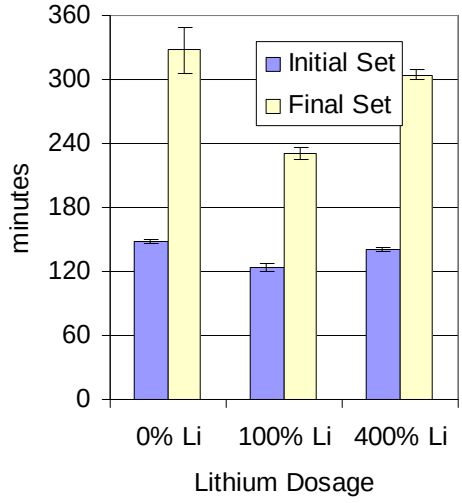

Figure 4.18. Vicat set times for Cement 2

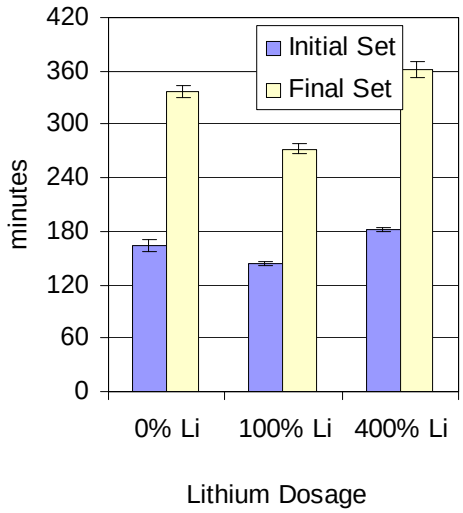

Figure 4.19. Vicat set times for Cement 3

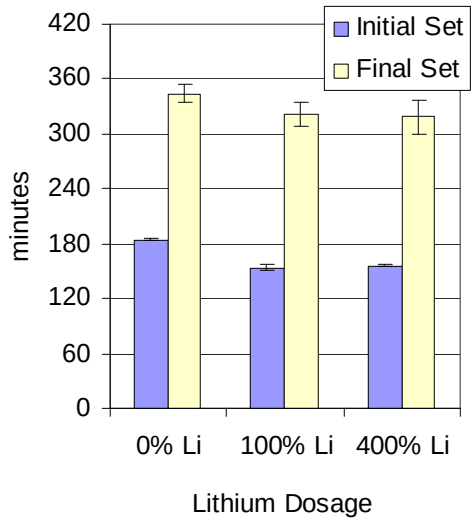

Figure 4.20. Vicat set times for Cement 4

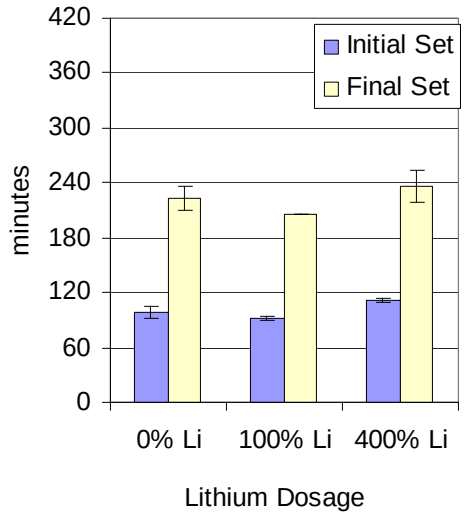

Figure 4.21. Vicat set times for Cement 5

4.4 Chemical Shrinkage

Chemical shrinkage, the absolute volume change of a hydrating cement, is approximately proportional to the extent of hydration. All six cements were examined, as well as the additional case of Cement 6 with fly ash replacement. Lithium was dosed at 0%, 100% and 400% for all cements, as well as at 50% and 200% for the Cement 6 mixes. As expected, results for chemical shrinkage on cement pastes in Figures 4.22 through 4.29 show trends similar to those obtained by calorimetry. Cements 1, 2, 3, and 5 show greater shrinkage in the first 24 hours of hydration with increasing lithium admixture dosage, presumably due to greater extent of reaction as indicated by calorimetry. The delay of shrinkage in the control mixes in these cements was indicative of the later hydration of these control mixes. Higher dosages showed chemical shrinkage earlier, indicating hydration acceleration. The hydration acceleration in this data is less apparent than in the calorimetry data, but it does in some cases confirm the acceleratory effect in the first 24 hours.

Cements 1, 2, 3, and 4 in Figures 4.22, 4.23, 4.24, and 4.25, respectively, show greater shrinkage after 24 hours by the control specimens. This corresponds to the trends observed by calorimetry in Figure 4.10, and Figures A.2, A.4, and A.5 in Appendix A. That is, although the lithium dosed mixes hydrate faster initially, within the first 24 hours the extent of hydration of the lithium mixes are surpassed by that of the control (no lithium) mix. This further suggests that lithium nitrate may accelerate hydration in the first 24 hours, but may retard hydration after 1 day.

Figures 4.28 and 4.29 illustrate chemical shrinkage data for Cement 6 with and without fly ash. Figure 4.28 shows greater initial shrinkage (greater early hydration) in

the lithium-dosed mixes, but does not clearly show a trend in shrinkage after 1 day as would be expected based on the calorimetry results. The effect of lithium on shrinkage in the first 24 hours is less apparent in Figure 4.29. This reinforces the conclusion from calorimetry testing that the effect of lithium in the first 24 hours is less noticeable in the presence of fly ash. Chemical shrinkage after 10 days in the Cement 6 pastes did not show any clear trends with lithium dosage.

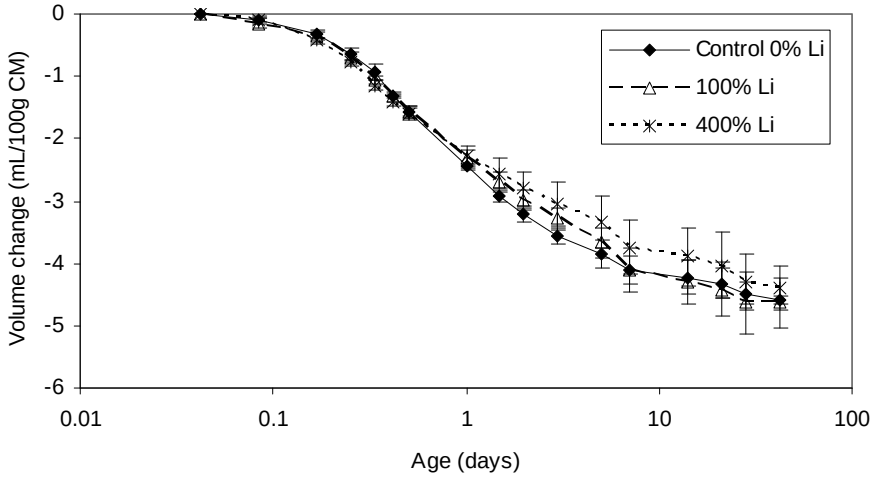

Figure 4.22. Chemical shrinkage results from Cement 1 (low alkali)

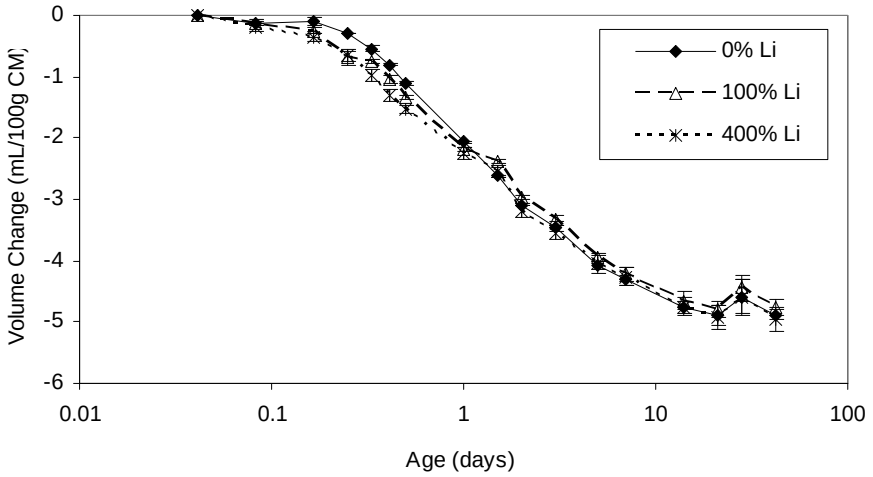

Figure 4.23. Chemical shrinkage results from Cement 2 (moderate alkali)

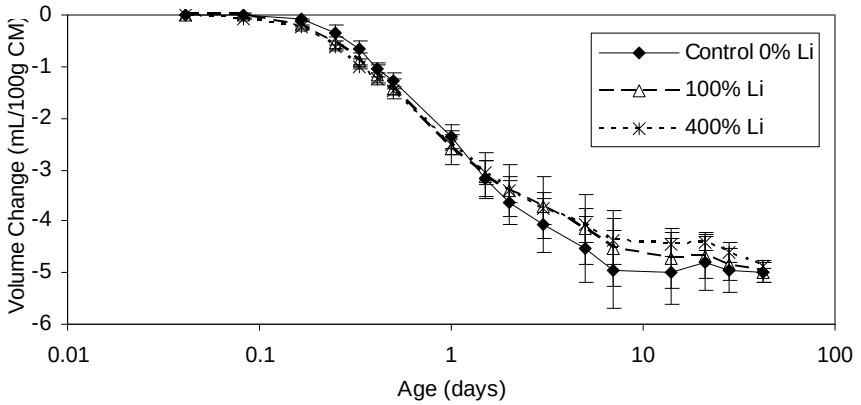

Figure 4.24. Chemical shrinkage results from Cement 3 (high alkali)

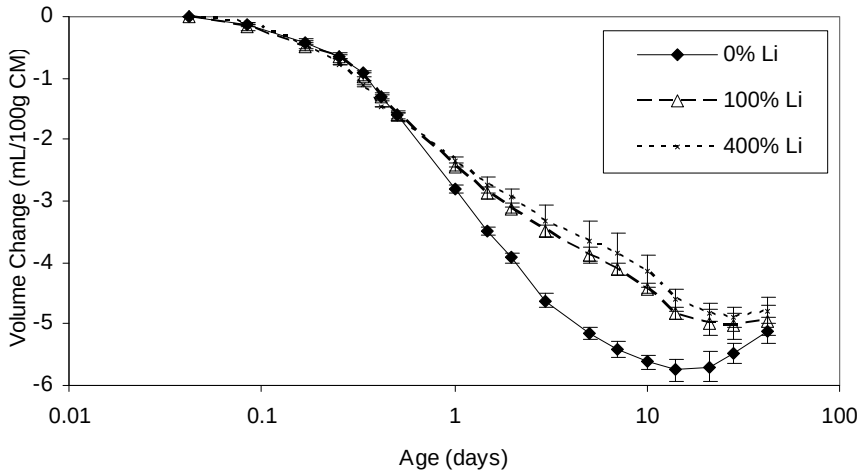

Figure 4.25. Chemical shrinkage results from Cement 4 (low C_3A).

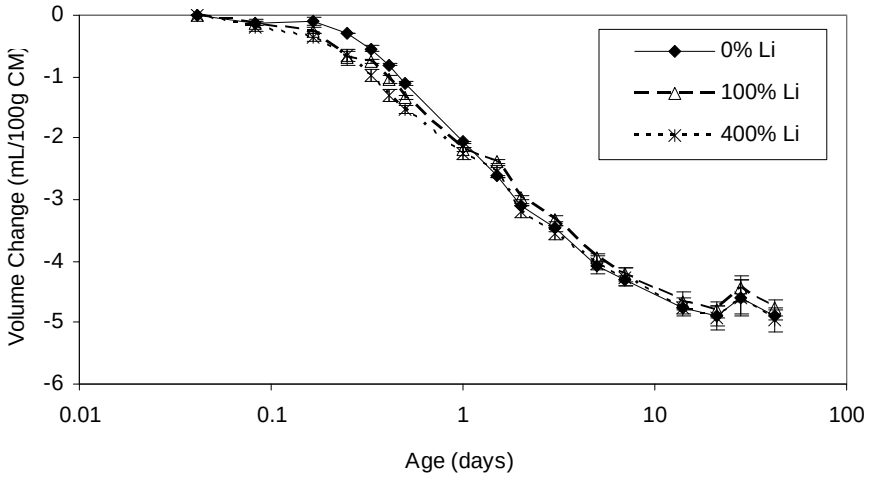

Figure 4.26. Chemical shrinkage results from Cement 2 (moderate C_3A).

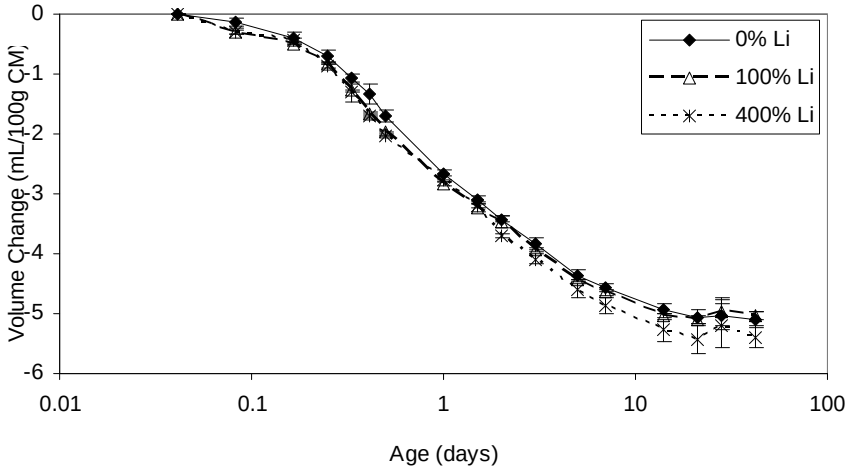

Figure 4.27. Chemical shrinkage results from Cement 5 (high C_3A)

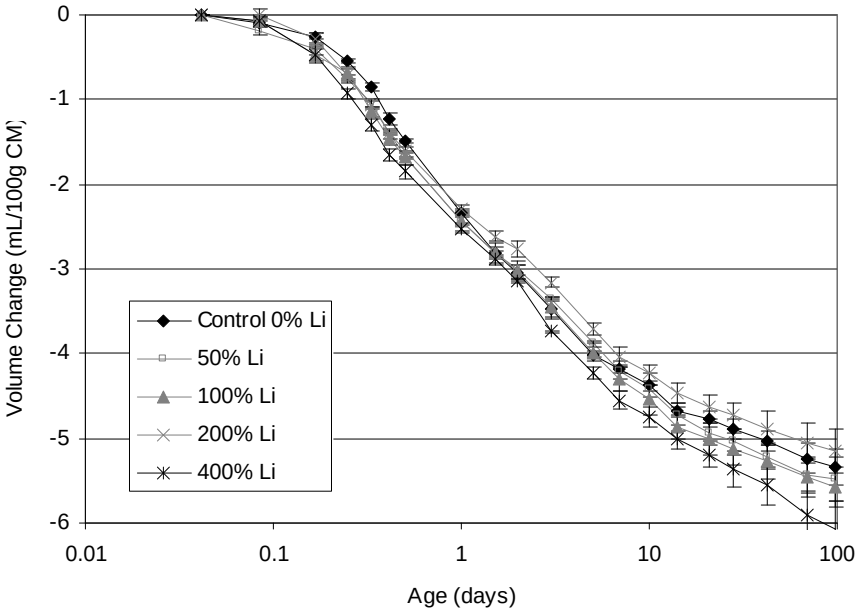

Figure 4.28. Chemical shrinkage results for Cement 6 with no fly ash.

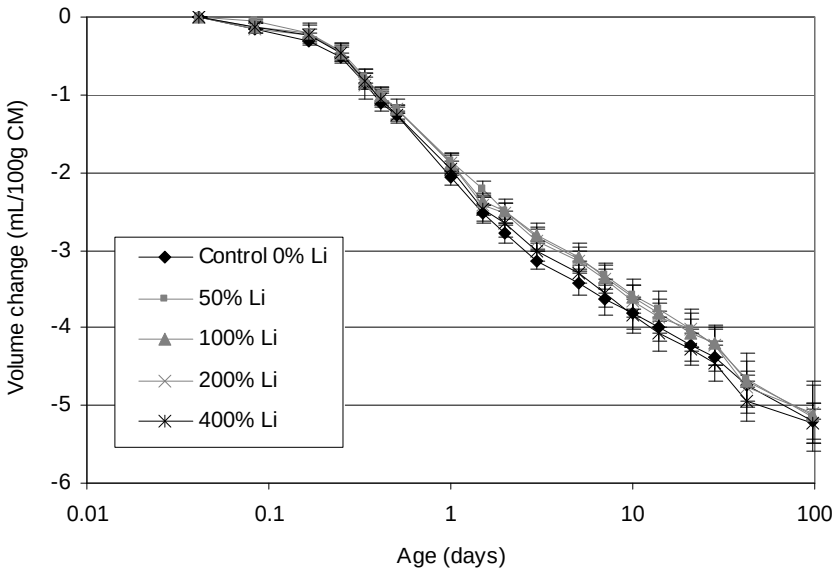

Figure 4.29 Chemical shrinkage results for Cement 6 with 20% fly ash replacement.

4.5 Autogenous Shrinkage.

Linear deformation due to autogenous shrinkage was measured in cement pastes cast in sealed, corrugated polymeric tubes by the method described by Jensen and Hansen (1995). While chemical shrinkage is an absolute volume change from the time of mixing, autogenous shrinkage is a measured linear deformation, measured after final setting, and is largely due to self desiccation in the capillary pores of the hydrating cement.

Effects of lithium nitrate on autogenous shrinkage were examined in all six cements, as well as the additional case of Cement 6 with fly ash replacement. Lithium was dosed at 0%, 100% and 400% for all cements, as well as at 50% and 200% for the Cement 6 mixes. Results are illustrated in Figures 4.30 through 4.36. Generally, as the lithium dosage increased, less autogenous shrinkage was observed in the first 10 days. Often, a net expansion occurred in the first 24 hours. In particular, Cement 4 in Figure 4.33 shows expansion at the 400% lithium dosage and shrinkage at 0% and 100% dosage.

After 28 days, pastes with the highest (400%) dosages exhibited significantly greater shrinkage than the control samples. However, in all conditions examined, pastes produced with the standard dosage of lithium nitrate (100% dosage) did not exhibit significantly more autogenous shrinkage than the corresponding control (no lithium) mixes.

Comparison of data for autogenous shrinkage in the Cement 6 pastes prepared with and without fly ash (Figures 4.35 and 4.36) shows no clear influence of fly ash replacement on the lithium effect on autogenous shrinkage. Overall shrinkage appears less in the fly ash mixes when compared to the cement alone, but the effects of lithium

appear the same in both. Both with and without fly ash replacement, the 400% dosage specimens exhibit more shrinkage after 28 days than other mixes.

Because similar increased post-28-day shrinkage is not evident in chemical shrinkage results in Figures 4.22 to 4.29, it is unlikely that further hydration of the 400% dosage mixes is responsible for this behavior. More likely, different development of microstructure and capillary pores in the 400% dosage mixes caused a different self-desiccation response to similar continued hydration of unreacted cementitious particles. Though similar quantities of water are consumed in the continued hydration of these 400% mixes (as shown by chemical shrinkage), because the capillary pore network is different, capillary tension (and hence autogenous shrinkage) develops differently.

Igarashi et al.(2005) has shown through the use of mercury intrusion porosimetry (MIP) and scanning electron microscope-backscattered electron image analysis (SEM-BSE) that mechanical properties of concrete , including autogenous shrinkage due to capillary tension, are dependent on total volume and connectivity of pores, and are particularly dependent on the volume of larger pores. Additionally, cement pastes have been shown to have a coarser microstructure and higher percentage of larger pores in pastes that have had hydration accelerated by addition of sodium hydroxide (NaOH) (Garci-Juenger, et al., 2001). This is not meant to imply that NaOH and $LiNO_3$ have the same effect on shrinkage, but rather to point out that acceleration of hydration has significant effects on the development of microstructure and the capillary pore network that affect autogenous shrinkage. In Garci-Juenger's (2001) research, acceleration comparable to that seen in Figures 4.1 to 4.6 of this chapter led to microstructural

differences in hydrated pastes, and also led to greater specimen shrinkage after 40 days as compared to control specimens.

The increased shrinkage in the 400% $LiNO_3$ dosage specimens for all cements is significant because autogenous shrinkage, occurring after final set, can induce tensile stresses in concrete. Higher tensile stresses in a concrete can cause cracking, and they also may increase the likelihood of localized ASR expansive forces causing cracking.

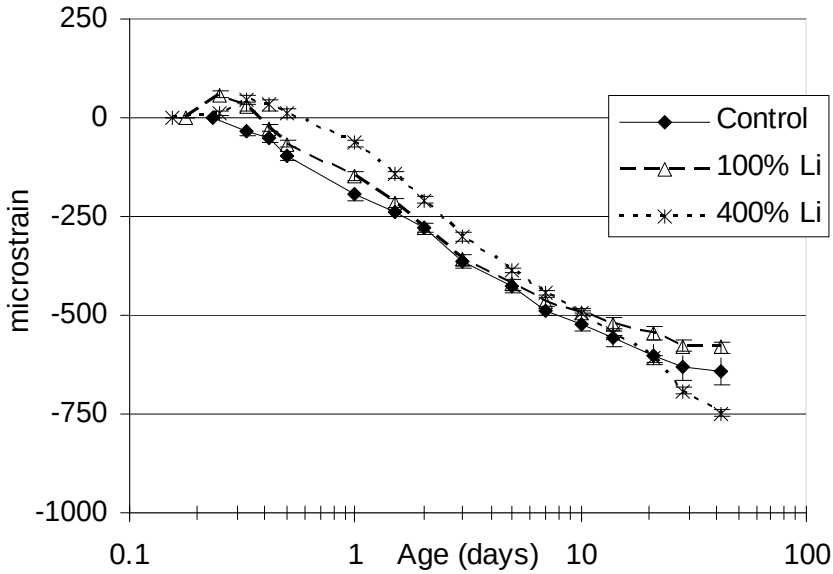

Figure 4.30 Autogenous shrinkage results for Cement 1.

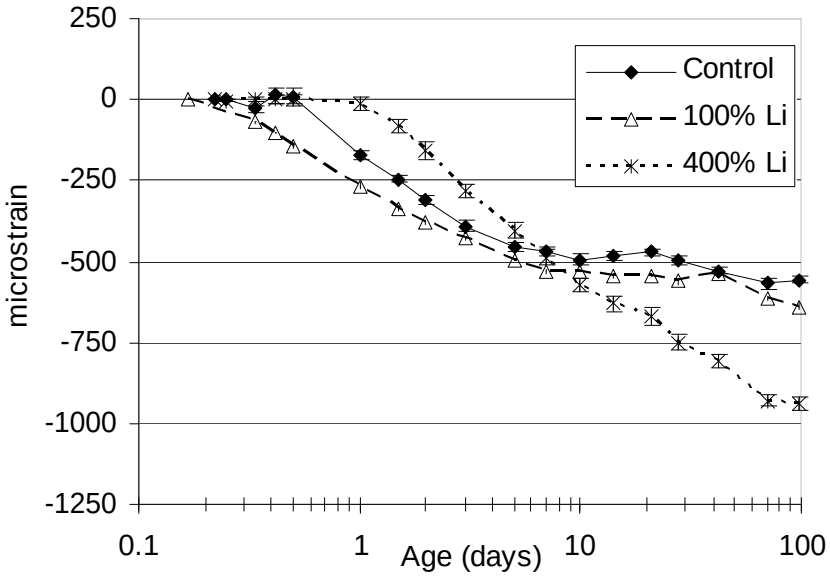

Figure 4.31. Autogenous shrinkage results for Cement 2.

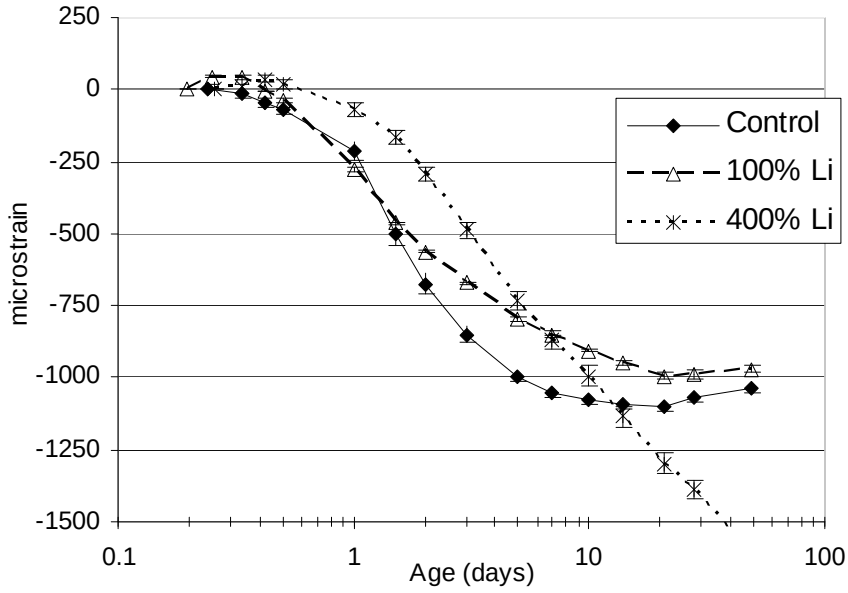

Figure 4.32. Autogenous shrinkage results for Cement 3.

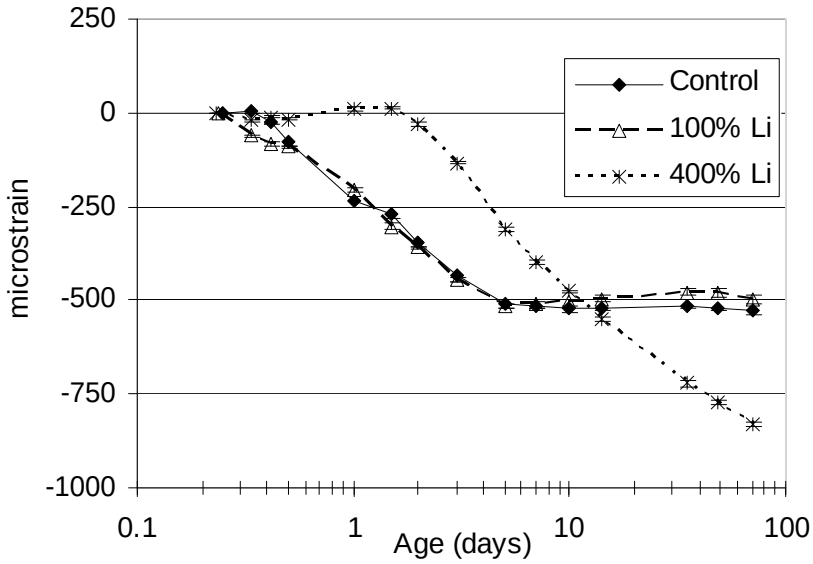

Figure 4.33. Autogenous shrinkage results for Cement 4.

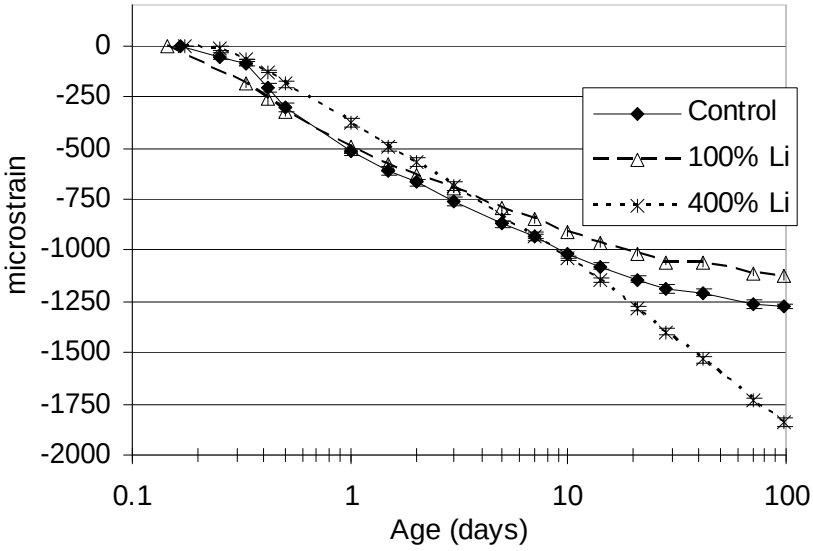

Figure 4.34. Autogenous shrinkage results for Cement 5.

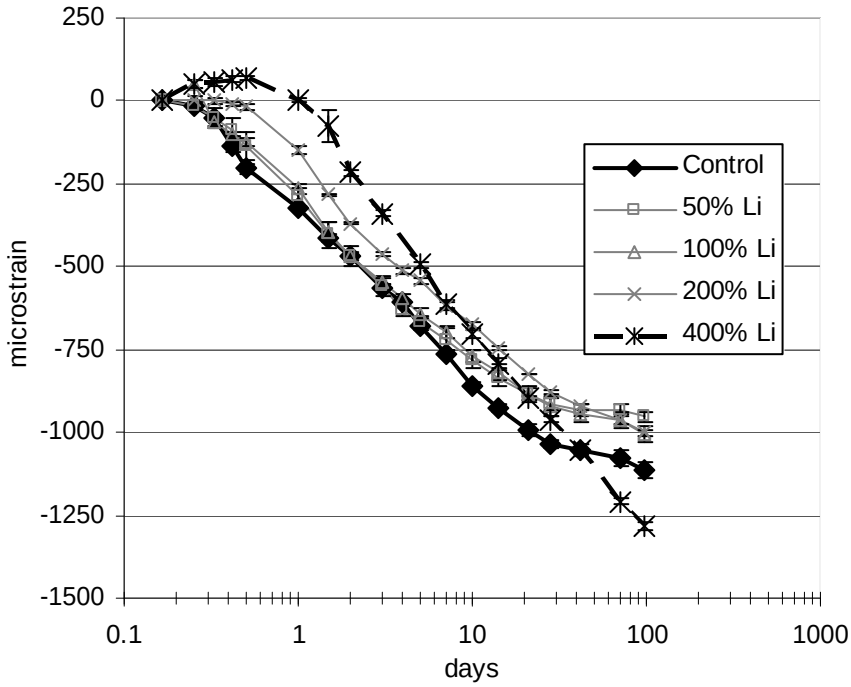

Figure 4.35. Autogenous shrinkage results for Cement 6 with no fly ash

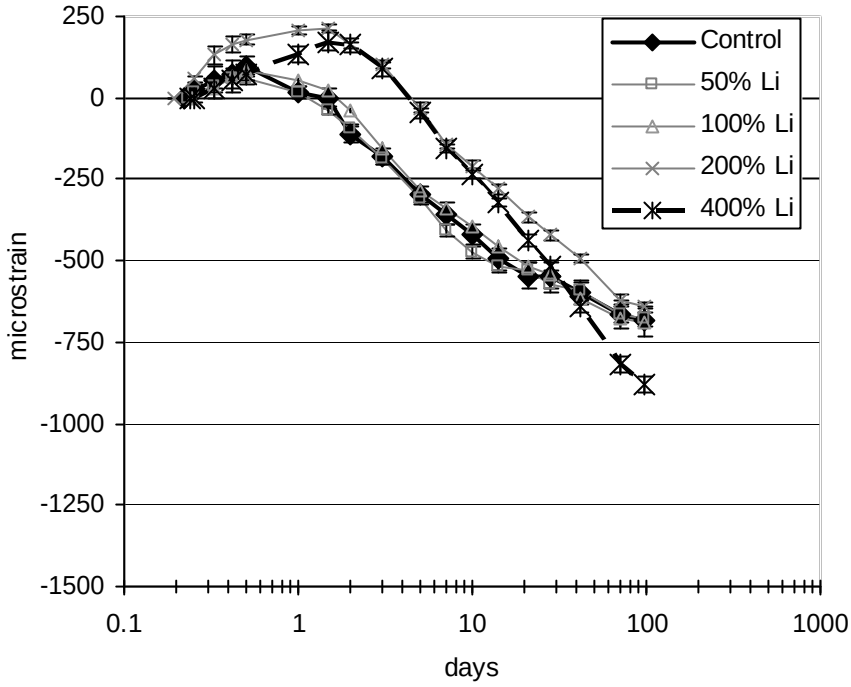

Figure 4.36. Autogenous shrinkage results for the Cement 6 with 20% fly ash replacement

4.6 Free Shrinkage

Linear deformation due to unrestrained shrinkage (combined autogenous and drying shrinkage) was measured in concrete prisms by a modified version of ASTM C 157. Specimens were measured starting at 24 hours, rather than lime-water curing for 28 days before measurements start as ASTM C 157 describes. Unlike the chemical and autogenous shrinkage tests, free shrinkage testing includes effects of drying and the restraining effects of aggregates. Effects of lithium nitrate on free shrinkage were examined using Cement 6, both alone and with 20% replacement by Class F fly ash. Lithium was dosed at 0%, 50%, 100%, 200%, and 400%. Results are illustrated in Figures 4.37 and 4.38. In free shrinkage data obtained from 1 through 28 days of age, no trends in effects of lithium dosage on behavior are apparent. Possibly due to additional variations introduced by the distribution and varying sizes of aggregates, the standard deviations in these results are higher than those in the tests on pastes only.

The free shrinkage data for the cement with fly ash in Figure 4.37 shows no significant difference in free shrinkage behavior between any of the dosages tested. The free shrinkage data for the cement alone (no fly ash) in Figure 4.38 shows less shrinkage in the 50% and 200% dosage specimens. The cause for this is unknown, but may have been due to varying curing conditions. These two mixes were performed on the same day and were cured simultaneously in the environmental chamber. The control, 100% and 400% specimens were mixed two weeks earlier, and curing conditions may have varied, although it is not clear how. Regardless, in the control, 100%, and 400% specimens, which were cured simultaneously, there is no significant difference in 28 day shrinkage values.

In the only previous study found on $LiNO_3$ effects on concrete shrinkage, Lane (2002) found that the standard dosage did not affect shrinkage of ASTM C 157 specimens observed for a period of one year. His tests, by allowing moist curing for 28 days before measurements began, effectively eliminated the first 28 days of the autogenous component of shrinkage from measured length changes. Apparently, while $LiNO_3$ appears to increase autogenous shrinkage in pastes after 28 days, this had little effect on the combined autogenous and drying components of shrinkage in Lane's concrete specimen tests. In both Lane's study and the current study, no effect of $LiNO_3$ was noted on free shrinkage of concrete specimens.

4.7 Restrained Shrinkage

Effects of lithium nitrate addition on restrained concrete age at cracking was investigated using restrained rings as described in ASTM C 1581. Effects of lithium nitrate were examined using Cement 6, both alone and with 20% replacement by Class F fly ash. Lithium was dosed at 0%, 50%, 100%, 200%, and 400%. Concrete rings were allowed to cure for 28 days, with shrinkage restrained by an inner steel ring. None of the rings cracked at any lithium dosage, with or without fly ash replacement, within 28 days. Since no trends were measured in the restrained shrinkage test, the potential for concrete cracking may be best evaluated using the free shrinkage results in Figures 4.37 and 4.38. These results appear to confirm that there is no clear evidence of an effect of lithium nitrate on concrete shrinkage at early ages (up to 28 days).

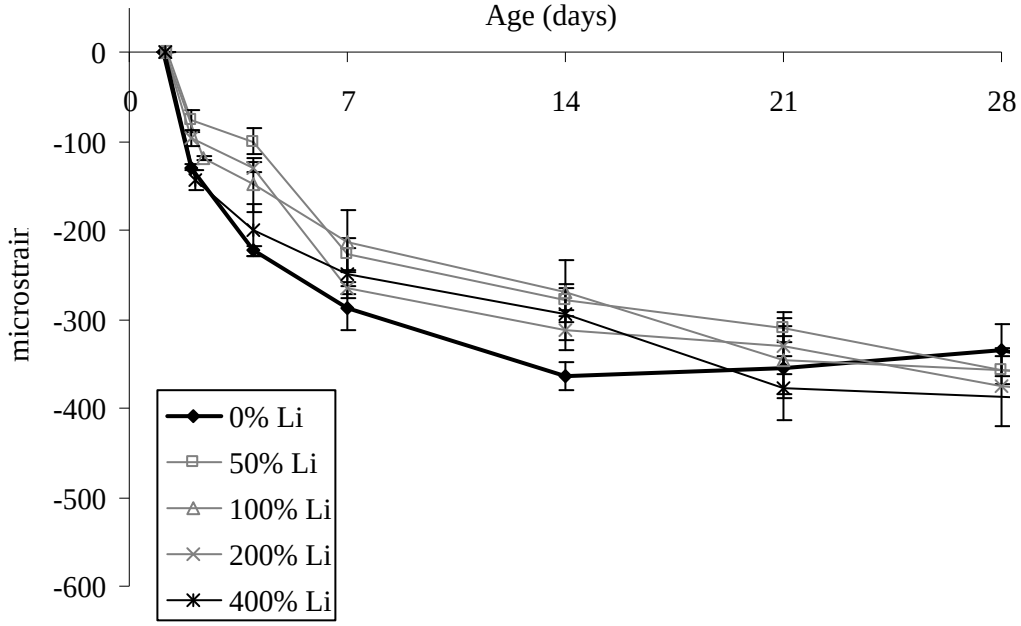

Figure 4.37. Free shrinkage results for concrete made from Cement 6 with 20% fly ash replacement

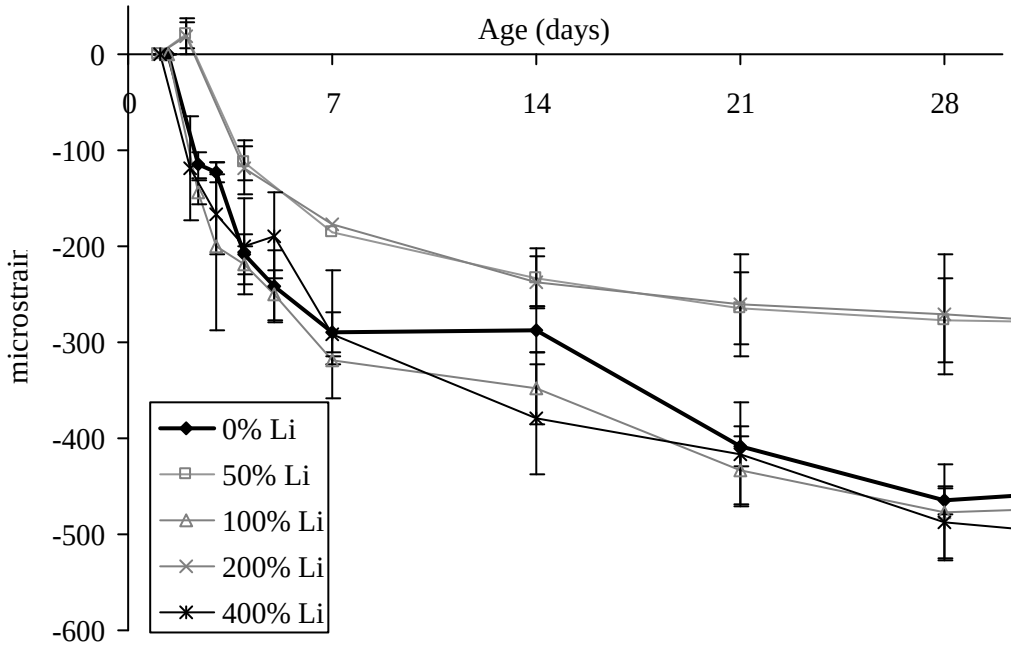

Figure 4.38. Free shrinkage results for concrete made from Cement 6 without fly ash

4.9 Strength

Effects of lithium nitrate addition on the compressive strength of concrete were investigated using concrete specimens made with Cement 6 with 20% Class F fly ash replacement, and $LiNO_3$ dosages of 0%, 50%, 100%, 200%, and 400%. Results in Table 4.3 are average and standard deviation values for five concrete cylinder specimens at each of five dosages. The trend of greater 28-day strengths at higher lithium nitrate dosages is evident in Figure 4.39. As compared to the control mix with no lithium, compressive strengths are 6% higher in the 100% dosage concrete and 15% higher in the 400% dosage concrete.

Analysis of variance indicates that the differences between the average compressive strengths are statistically significant. That is, the variations within each batch were relatively small compared to the differences between batches with different dosages. Table 4.4 shows a p-value of 2.2% for comparison of the 100% dosage to the control specimen strengths, and Table 4.5 shows 0.0036% for comparison of the 400% dosage to the control specimen strengths. This means that there is only a 2.2% chance that the Control and the 100% dosage mixes were of the same strength, and there is less than 0.01% chance that the Control and 400% batches were of equal strength. This analysis is based on variations between specimens in each batch, but does not consider expected batch-to-batch variations. Analysis of variance including batch-to-batch variations would require specimens from more than one batch at each dosage.

Table 4.3. 28-day compressive strengths of lab specimens batched at Georgia Tech, w/cm=0.30, 20% Class F fly ash replacement, average of 5 cylinders .

$LiNO_3$ Dosage	**0%**	**50%**	**100%**	**200%**	**400%**
Average Compressive Strength (psi)	6909	7617	7361	7473	7960
Standard Deviation (psi)	266	241	239	293	106

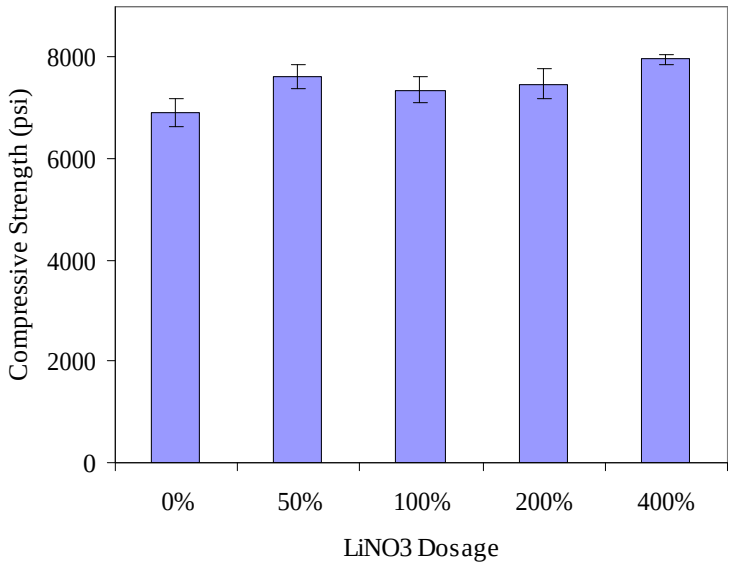

Figure 4.39. 28-day compressive strengths of lab specimens batched at Georgia Tech, w/cm=0.30, 20% Class F fly ash replacement, average of 5 cylinders.

Table 4.4. ANOVA table for 100% dosage vs Control compressive strength

	Degrees of Freedom	Sum of Squares	Mean Squares	F-statistic	p-value
Lithium Dosage	1	510199	510199	7.974	2.24%
Error	8	511892	63986		
Total	9	1022090			

Table 4.5. ANOVA table for 400% dosage vs Control compressive strength

	Degrees of Freedom	Sum of Squares	Mean Squares	F-statistic	p-value
Lithium Dosage	1	2762105	2762105	67.337	0.0036%
Error	8	328151	41019		
Total	9	3090257			

Results of additional tests on effects of lithium nitrate on concrete strength performed by an outside laboratory on concrete specimens cast in the field during the reconstruction of Ramps 1 and 2 at H-JAIA are not in agreement with these tests performed at Georgia Tech. Results from compressive and flexural strength tests of concrete specimens made from full-scale construction mixes using Cement 6 with Class F fly ash, and with varying lithium dosages, are shown in Appendix C. Average compressive strength values were 8% lower at the 200% $LiNO_3$ dosage, and 15% lower at the and 400% $LiNO_3$ dosage, as compared to the control mix. These results indicate lower compressive strengths at increasing dosages, contradicting results from Georgia Tech lab testing. Airport flexural strength values showed lower strength for the control

specimens and higher strength at the 400% dosage, but no clear trend at intermediate dosages.

Results of further strength testing carried out on mortar cubes by Xavier Joudain at Georgia Tech are included in Appendix D. These mortar cubes were made from Cement 6, with and without 20% Class F fly ash replacement, and tested at 28 days. No clear trend of $LiNO_3$ effects on compressive strengths of these mortar cubes is apparent.

Acceleration of hydration, such as the acceleration seen in Section 4.1 of this Chapter, has been shown to have negative effects on 28-day strength (Garci-Juenger, 2001). Additionally, effects of $LiNO_3$ on the cement matrix microstructure described in Section 4.5 would be expected to affect strength. However, previous research using $LiNO_3$ described in Chapter 2 found no discernable significant effect on strength, (Thomas et al., 2003; McKeen et al., 2000). These previous studies were performed at lower admixture dosages than explored in the current study. Regardless, strength data collected in this research is in some cases inconsistent, and is similarly inconclusive.

CHAPTER V

Conclusions

Through this research, the effects of lithium nitrate ($LiNO_3$) on early age concrete behavior were investigated. A summary of the findings of this research and recommendations for future research follow.

5.1 Research Findings

Isothermal calorimetry results indicate that the 30% by weight $LiNO_3$ admixture tested accelerates the hydration of the tricalcium silicate (C_3S) and tricalcium aluminate (C_3A) components of cement, generating more early heat than control mixes. This is illustrated by the shift upward and to the left of both peaks in the calorimetry curves, for increasing $LiNO_3$ dosages. This acceleration relative to the control mixes was observed in all cements tested, and at all dosages. Additionally, lower alkali cements, which are more likely to be specified in applications where ASR is a concern, appear more susceptible to this acceleration. Calorimetry results suggest that lithium ions in the mix water may behave similarly to sodium (Na^+) and potassium (K^+) ions. All three are Group 1 alkalis and accelerate C_3S hydration likely by reducing the solubility of calcium-containing hydration products in the saturated mix water, thereby advancing nucleation. Acceleration of the C_3A component may be due to lithium aiding in the dissolution of C_3A; other Group 1 alkalis have shown this behavior.

Comparison of calorimetry results for cements of various alkali contents suggests that acceleration effects of lithium, sodium, and potassium are additive. Addition of

lithium to low alkali cements, then, causes a larger relative increase in the combined [Li^+ + Na^+ + K^+] concentration, causing greater acceleration than in high alkali cements. Although the lithium sensitivity of a cement likely depends on more variables than just alkali content, alkali content is likely a factor.

This acceleration, and the increase in early heat generation, may be harmful in some concrete applications where high temperatures are a concern. However, calorimetry results also indicate that the inclusion of Class F fly ash at 20% by weight replacement of cement appears to diminish these possibly negative effects of $LiNO_3$ on early age hydration acceleration and heat generation. As Class F fly ash has ASR-mitigating effects of its own, its use in applications where lithium nitrate is specified is likely.

Acceleration of the C_3A peak, which is deliberately delayed by addition of gypsum in the manufacture of cement, is expected to affect concrete workability, set time, and strength. However, the standard dosage of $LiNO_3$ produced no significant change in concrete rheological parameters, and only a slight increase in slump. Higher dosages appeared to slightly decrease the Bingham yield stress, and may increase viscosity, of fresh concrete. No bleed water effect was observed for any $LiNO_3$ dosage.

In addition, the times of initial and final setting of paste specimens were only affected in one of the six cements tested. In this lowest alkali cement (Na_2O_e = 0.295%), initial and final set times were decreased by 15% and 22%, respectively. It may be significant that the only cement to be affected by the lithium nitrate admixture was the lowest alkali cement, and that calorimetry testing suggested that lower alkali cements are more susceptible to hydration reaction acceleration. It is significant in these results that

none of the negative behaviors associated with C_3A acceleration were observed at lithium dosages up to four times the standard effective dosage. There was no indication of early stiffening or flash-set at any dosage, and the reduction in set time for the low alkali cement appears manageable from a construction viewpoint.

In autogenous shrinkage testing, higher $LiNO_3$ dosages appeared to cause initial expansion in some sealed paste specimens, possibly due to ettringite formation. However, with all cements, and with the cement with fly ash replacement, the highest dosage (400% of the standard dosage) of $LiNO_3$ led to greater autogenous shrinkage after 40 days. The increased autogenous shrinkage in the 400% dosage specimens for all cements is significant because shrinkage, occurring after final set, can induce tensile stresses in concrete. Higher tensile stresses in a concrete structure can cause cracking, and also may increase the likelihood of localized ASR expansive forces causing cracking.

In concrete free shrinkage specimens, however, the restraining effect of aggregates diminished shrinkage, and no effect of the $LiNO_3$ was apparent. Additionally, in no cases, with any dosage of lithium tested, with or without fly ash replacement, did restrained shrinkage specimens show any cracking.

Results from strength testing were inconclusive. The average compressive strength of laboratory-cast specimens increased with greater amounts of $LiNO_3$, but the average compressive strength of field–cast cylinders decreased with increasing $LiNO_3$ dosages. Laboratory-cast mortar cube compression testing showed no clear trends with strength and admixture dosage. Negative 28-day strength effects typically associated with acceleration of the C_3A hydration reactions shown in calorimetry were not evident in the laboratory-cast samples, although lower strengths were noted in the field-cast

samples. Further research is necessary to conclusively understand the implications of $LiNO_3$ effects on concrete strength.

Based upon these results, a maximum $LiNO_3$ dosage of 100% is recommended for practical use. At the 200% $LiNO_3$ dosage negative strength effects were observed in the Hartsfield-Jackson Atlanta International Airport reconstruction project specimens. At the 400% $LiNO_3$ dosage negative effects were observed in the autogenous component of shrinkage for all cements. Without further study to clarify strength effects and to determine the significance of the observed shrinkage effects, these higher dosages may negatively affect concrete properties.

5.2 Recommendations for Future Research

If, due to the potential detrimental effects of new de-icing chemicals on concrete airfield pavements, the use of higher than the current standard dosage $LiNO_3$ is to be considered, further investigation into effects of higher (i.e., >100%) dosages of lithium admixtures on concrete behavior are warranted. In particular, further examination of the influence of lithium admixtures on shrinkage is recommended. Although this research showed no effect of $LiNO_3$ on drying shrinkage in free and restrained concrete testing, the autogenous component of shrinkage showed increases at the 400% dosage rate for all cements tested. The potential for shrinkage cracking is dependent on the interaction of these drying and autogenous components of shrinkage. Specimen geometry, the shrinkage-restraining effect of aggregate, and relative humidity play significant roles in this interaction, and should be considered in future study.

Further research is also necessary for conclusive evidence of $LiNO_3$ effects on concrete strength. Results in this research were inconclusive and in some cases contradictory. Further strength testing should be limited to a controlled environment, and should consider several cements of different compositions.

Longer-duration calorimetry in conjunction with strength testing could be used to determine the significance of the larger cumulative heats generated by the hydration of lithium mixes. Additionally, low alkali cements in particular (likely to be used with lithium in the field) could be examined for other negative effects associated with hydration acceleration. Cements that show more severe acceleration with $LiNO_3$ dosing likely develop different microstructure and capillary pore networks with lithium dosing. These cements may show the most severe effects of $LiNO_3$ on long term shrinkage. Since creep in concrete is also dependant on the capillary pore network, investigations into creep behavior may reveal $LiNO_3$ effects.

Microstructural effects of lithium could also be investigated using nitrogen absorption, quantitative X-Ray diffraction (QXRD), mercury intrusion porosimetry (MIP), or scanning electron microscope-backscattered electron image analysis (SEM-BSE).

$LiNO_3$ appears to affect the timing of the C_3A hydration reactions. Since the timing of the hydration of this cement component is also dependent on cement sulfate content, cements with different sulfate contents may be affected differently by $LiNO_3$. Investigation of sulfate content and $LiNO_3$ dosing interactions may provide more understanding on the observed $LiNO_3$ acceleration of C_3A hydration reactions.

Due to the low w/c in this study, no bleed water was observed at any $LiNO_3$ dosage. Investigation at higher water contents may be more likely to reveal $LiNO_3$ effects. Additionally, further slump and rheology testing may clarify the possible effects observed in this study, particularly if measures are taken to minimize data scatter. Rheology testing using smaller aggregates or mortar only may decrease data scatter.

APPENDIX A

Calorimetry Cumulative Heat Evolved Graphs for Cements 1 through 5

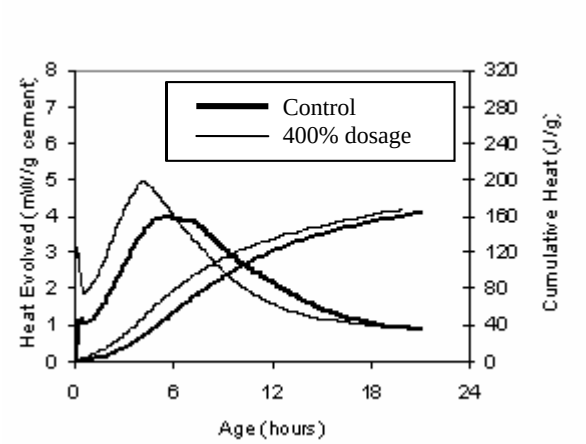

Figure A.1 Cumulative Heat Evolved, Cement 1,
Control and 400% $LiNO_3$ dosage mixes.

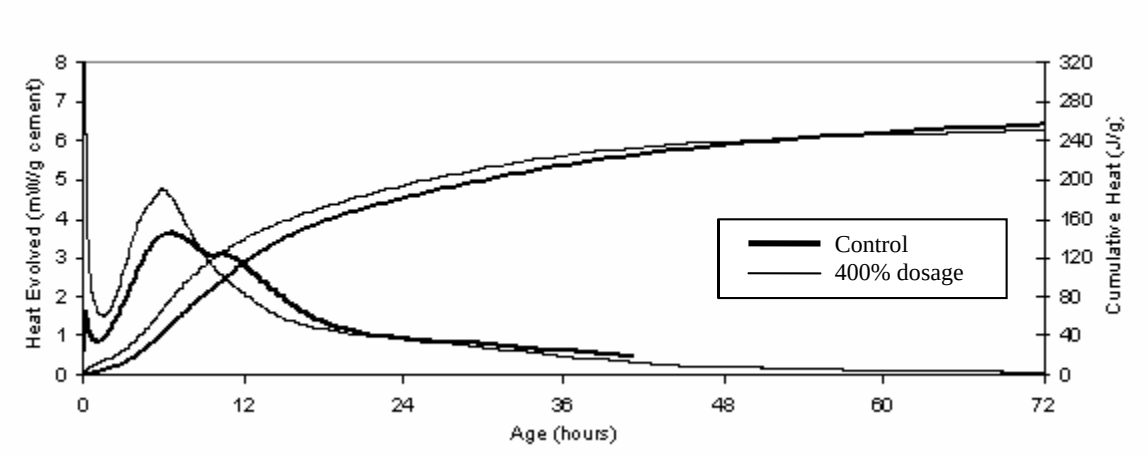

Figure A.2 Cumulative Heat Evolved, Cement 2,
Control and 400% $LiNO_3$ dosage mixes.

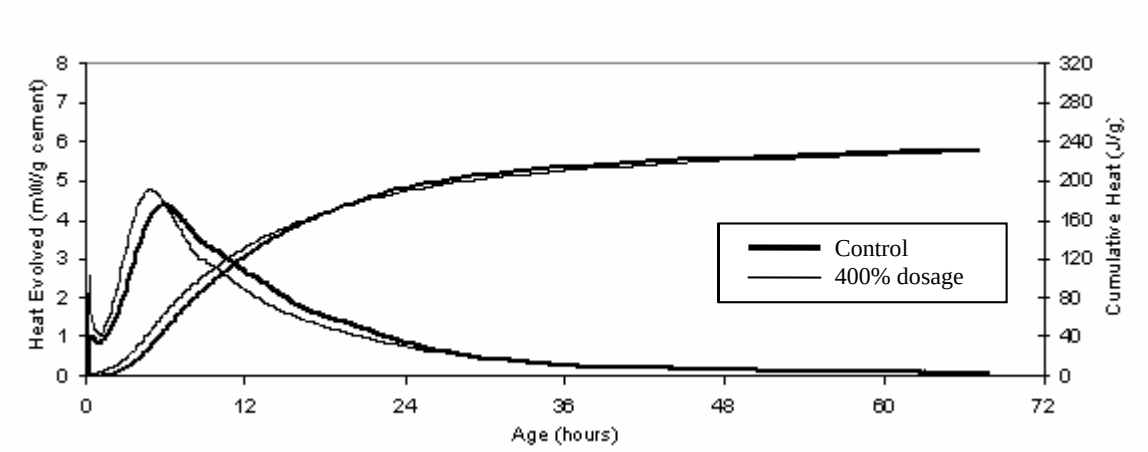

Figure A.3 Cumulative Heat Evolved, Cement 3,
Control and 400% $LiNO_3$ dosage mixes.

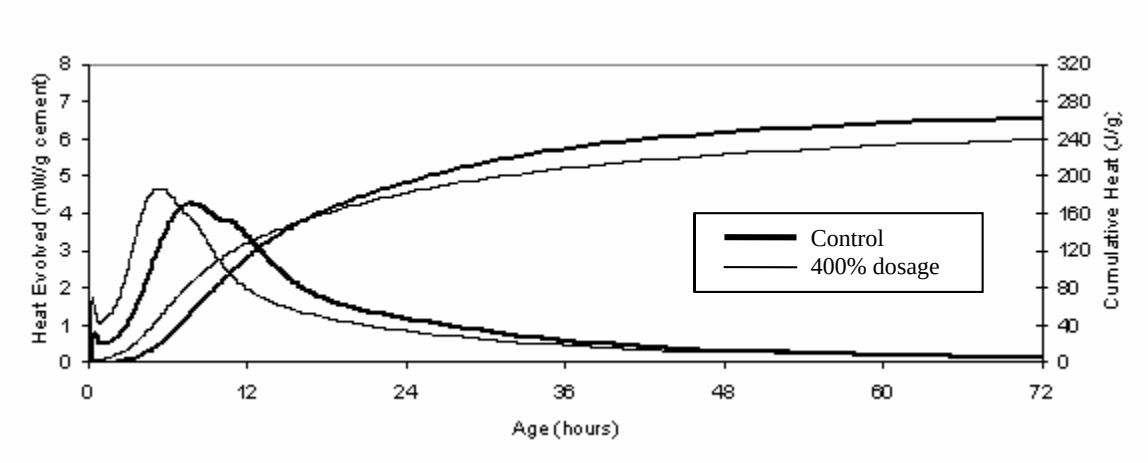

Figure A.4 Cumulative Heat Evolved, Cement 4,
Control and 400% $LiNO_3$ dosage mixes.

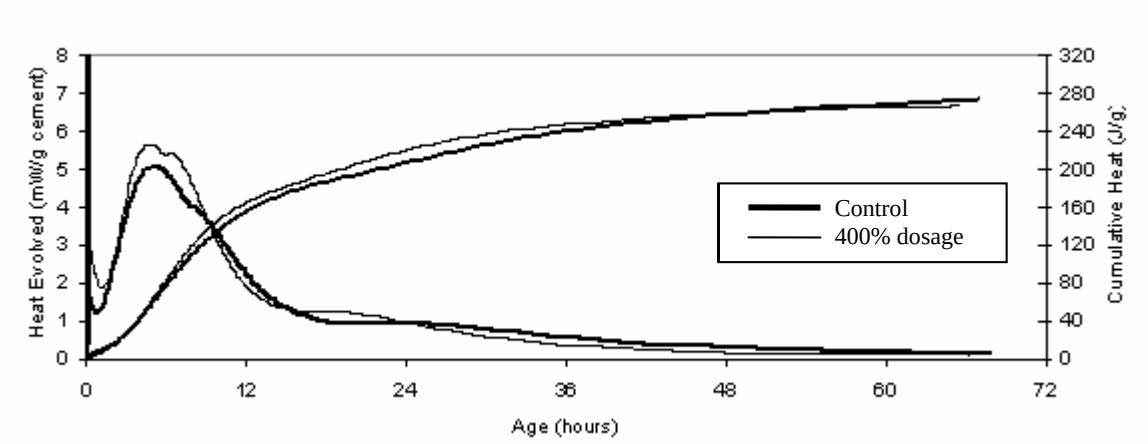

Figure A.5 Cumulative Heat Evolved, Cement 5,
Control and 400% $LiNO_3$ dosage mixes.

APPENDIX B

High Temperature Vicat Time of Setting Test Results

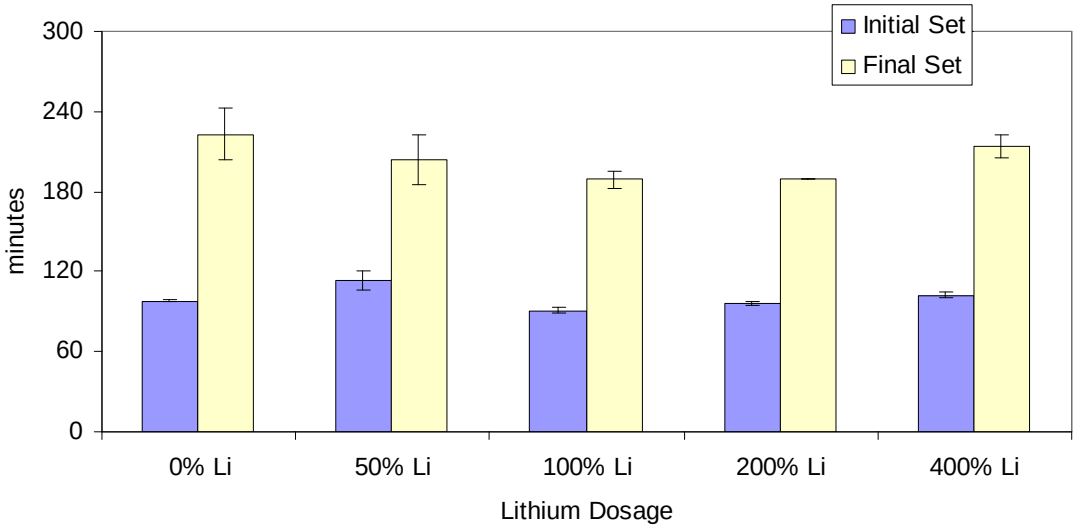

Figure B.1. Vicat setting times for Cement 6 with no fly ash.

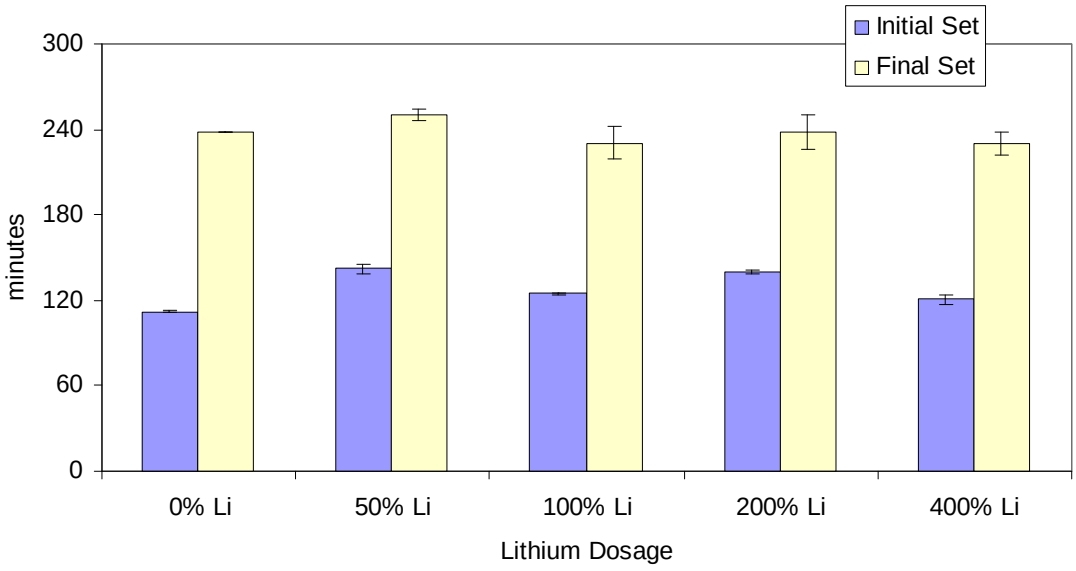

Figure B.2. Vicat setting times for Cement 6 with 20% Class F fly ash replacement

APPENDIX C

Strength Results from Hartsfield-Jackson Atlanta International Airport Ramps 1 and 3 Reconstruction

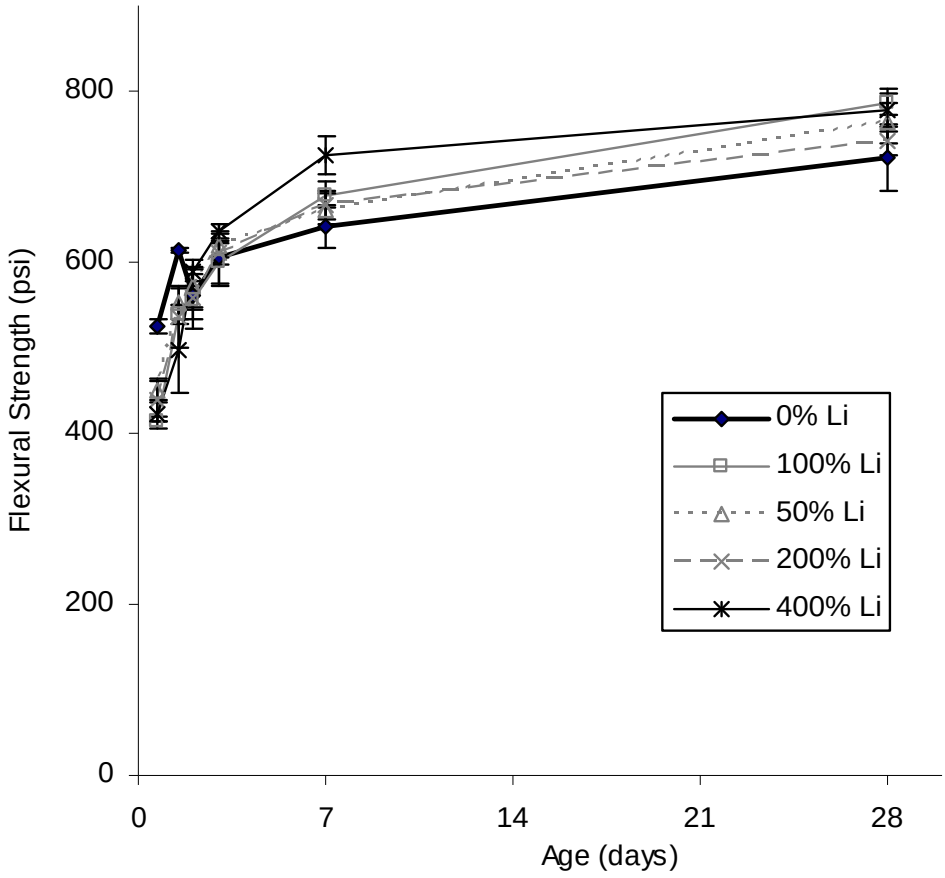

Figure C.1 Flexural strength development of full-scale production batches using Cement 6 with 20% Class F fly ash replacement, reported by outside consultant.

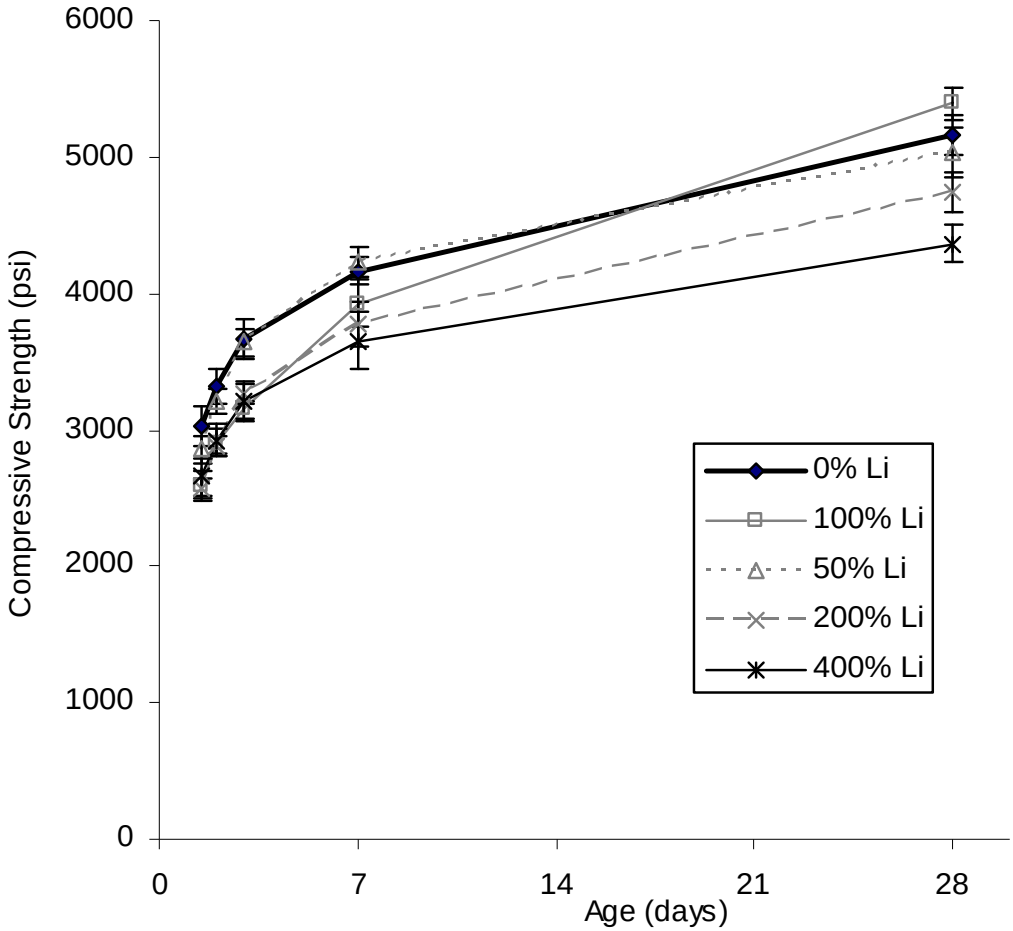

Figure C.2. Compressive strength development of full-scale production batches using Cement 6 with 20% Class F fly ash replacement, reported by outside consultant.

Table C.1 Oxide analysis of Cement 6 batches used for lab testing at Georgia Tech, vs. for H-JAIA batches.

	GT Lab tests	Outside tests
SiO_2 (%)	20.06	20.45
Al_2O_3 (%)	4.89	4.66
Fe_2O_3 (%)	3.00	3.06
CaO (%)	64.22	62.98
MgO (%)	2.68	3.71
SO_3 (%)	2.74	2.58
Na_2O (%)	0.115	0.087
K_2O (%)	0.444	0.425
NaO_2 Equiv. (%)	0.407	0.32
P2O5 (%)	0.076	0.071
TiO_2 (%)	0.274	0.28
SrO (%)	0.038	0.039
Mn_2O_3 (%)	0.088	0.125
Cr_2O_3 (%)	0.012	0.014
LOI (%)	1.37	1.52
C_3S (%)	64.1	58
C_2S (%)	9.2	15
C_3A (%)	7.9	7
C_4AF (%)	9.1	9

APPENDIX D

Compressive Strength Results from Mortar Cube Tests

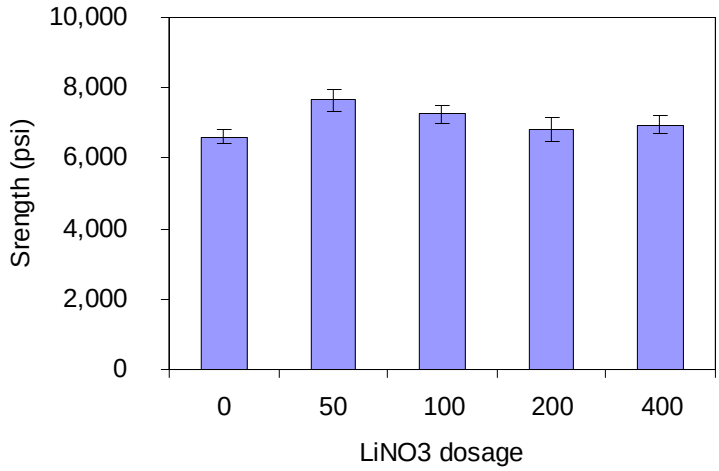

Figure D.1. Compressive strength of mortar cubes made with Cement 6 and no fly ash.

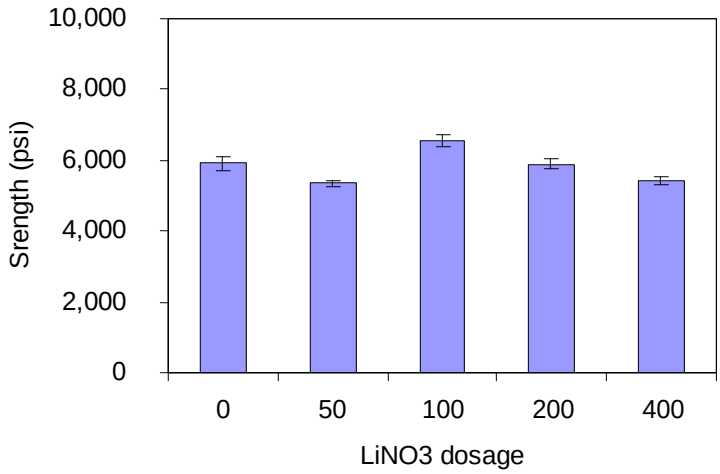

Figure D.2. Compressive strength of mortar cubes made with Cement 6 and 20% Class F fly ash replacement.

REFERENCES

1. American Society for Testing and Materials. *Standard Test Method for Compressive Strength of Cylindrical Concrete Specimens*. ASTM Designation C 39-05. West Conshohocken, PA. 2005.

2. American Society for Testing and Materials. *Standard Test Method for Flexural Strength of Concrete (Using Simple Beam with Third-Point Loading).* ASTM Designation C 78-02. West Conshohocken, PA. 2002.

3. American Society for Testing and Materials. *Standard Test Method for Slump of Hydraulic-Cement Concrete*. ASTM Designation C 143-05. West Conshohocken, PA. 2005.

4. American Society for Testing and Materials. *Standard Test Method for Length Change of Hardened Hydraulic-Cement Mortar and Concrete*. ASTM Designation C 157-04. West Conshohocken, PA. 2004.

5. American Society for Testing and Materials. *Standard Practice for Mechanical Mixing of Hydraulic Cement Pastes and Mortars of Plastic Consistency*. ASTM Designation C 305-99. West Conshohocken, PA. 1999.

6. American Society for Testing and Materials. *Standard Practice for Making and Curing Concrete Test Specimens in the Laboratory*. ASTM Designation C 192-05. West Conshohocken, PA. 2005.

7. American Society for Testing and Materials. *Standard Test Method for Bleeding of Concrete.* ASTM C Designation 232-04. West Conshohocken, PA. 2004.

8. American Society for Testing and Materials. *Standard Test Method for Time of Setting of Hydraulic Cement by Vicat Needle.* ASTM Designation C 191-04b. West Conshohocken, PA. 2004.

9. American Society for Testing and Materials. *Standard Test Method for Determining Age at Cracking and Induced Tensile Stress Characteristics of Mortar and Concrete under Restrained Shrinkage*. ASTM Designation C 1581-04. West Conshohocken, PA. 2004.

10. American Society for Testing and Materials. *Standard Test Method for Chemical Shrinkage of Hydraulic Cement Paste*. ASTM Designation C 1608-05. West Conshohocken, PA. 2005.

11. American Society for Testing and Materials. *Standard Test Method for Potential Alkali Reactivity of Aggregates (Mortar-Bar Method)* ASTM Designation C 1260-05. West Conshohocken, PA. 2005.

12. American Society for Testing and Materials. *Standard Test Method for Determination of Length Change of Concrete Due to Alkali-Silica Reaction* ASTM Designation C 1293-01. West Conshohocken, PA. 2001.

13. Berubé, M.A., Tramblay, C., Fournier, B., Thomas, M.D., and Stokes, D.B. "Influence of Lithium-based Products Proposed for Counteraction ASR on the Chemistry of Pore Solution and Cement Hydrates", *Cement and Concrete Research*, V. 34, 2004, p. 1645.

14. Bhaty, M.S.Y. and Greening, N.R., *Proc. 4th International Conference on Alkali-Aggregate Reaction*, Purdue, Indiana, 1978, p.87.

15. Carse, A. "Review of the Present Condition of the Lucinda Bulk Sugar Terminal at Lucinda in North Queensland Australia", *Proceedings of the 12th International Conference on Alkali-Aggregate Reaction in Concrete*, Beijing, p. 1025-1034, 2004.

16. Collins, C.L., Ideker, J.H., and Kurtis, K.E. "Laser Scanning Confocal Microscopy for *In Situ* Monitoring of Alkali-Silica Reaction," *Journal of Microscopy*, V.213, Feb 2004, p.149-157.

17. Diamond, S. "Unique Response of $LiNO_3$ as an Alkali Silica Reaction-Preventive Admixture," *Cement and Concrete Research*, Vol. 29, p. 1271-1275, 1999.

18. Diamond, S. and S. Ong. "The Mechanisms of Lithium Effects on ASR," *Proceedings of the 9th International Conference on Alkali-Aggregate Reaction in Concrete*, London, p. 269-278, 1992.

19. Du, L. and Folliard, K.J. "Mechanisms of Air Entrainment in Concrete", *Cement and Concrete Research*, in press.

20. Durand, B. (2000). "More Results about the Use of Lithium Salts and Mineral Admixtures to Inhibit ASR in Concrete," *Proceedings of the 11th International Conference on Alkali-Aggregate Reaction (ICAAR)*, Quebec, Canada, June 11-16, 623-632.

21. FMC Lithium Lifetime N Admixture Data Sheet, FMC Corp. 2001. http://www.fmclithium.com/products/pds/LifetimeN.pdf

22. Folliard, K.J., Thomas M.D., Kurtis, K.E., "Guidelines for the Use of Lithium to Mitigate or Prevent ASR", FHWA Report: FHWA-RD-03-047, July 2003.

23. Gajda, J. "Development of a Cement to Inhibit Alkali-Silica Reactivity", PCA Research and Development Bulletin RD 115T, Skokie, Illinois, 1996.

24. Garci Juenger, M. C., and Jennings, H.M. "Effects of High Alkalinity on Cement Pastes", *ACI Materials Journal*, V. 98, No. 3, May-June, 2001, p. 251.

25. He, Z. and Li, Z. "Influence of Alkali on Restrained Shrinkage Behavior of Cement-based Materials", *Cement and Concrete Research*, V.35, 2005, p.457-463.

26. Hewlett, Peter C. *Lea's Chemistry of Cement and Concrete*, 4th ed., London: Arnold 1998; pp.874-875.

27. Hooper, R.L., Morlidge, J., Lardner, K., and Thomas, M.D.A. "Use of Lithium Compounds to Prevent Damaging ASR in Concrete", BR426, CRC Ltd., London, 2001.

28. Hooper, R.L., Nixon, P.J., and Thomas, M.D.A., "Considerations When Specifying Lithium Admixtures to Mitigate the Risk of ASR", *Proceedings of the 12th International Conference on Alkali-Aggregate Reaction in Concrete*, (Eds. T. Mingshu and D. Min), International Academic Publishers/World Publishing Corp., Beijing, 2004, Vol. I, p.554-563.

29. Igarashi, Shin-ichi, A. Watanabe, M. Kawamura. "Evaluation on Capillary Pore Size Characteristics in High-strength Concrete at Early Ages", *Cement and Concrete Research*, V.35, 2005, p.513-519.

30. Jawed, Inam, and Jan Skalny. "Alkalies in Cement: A Review", *Cement and Concrete Research*, Vol. 8, pp. 37-52, 1978.

31. Jensen, O. Mejlhede, and Hansen, P. Freiesleben "A Dilatometer for Measuring Autogenous Deformation in Hardening Portland Cement Paste", *Materials and Structures*, 1995, V. 28, pp 407-409.

32. Johnson, D. "Mitigation of Potential Alkali-silica Reactivity Using Lithium", SHRP Concrete and Structures ASR Showcase Test and Evaluation Project 34, Study SD95-21, Interim Report, South Dakota Department of Transportation, May 1997.

33. Kasmatka, Steven H., Beatrix Kerkhoff, William C. Panarese. Design and Control of Concrete Mixtures, Portland Cement Assosciation, 14th ed. 2005, Skokie, IL.

34. Lane, D.S. "Laboratory Investigation of Lithium-bearing Compounds for use in Concrete", VTRC 02-R16, Virginia Transportation Research Council, Commonwealth of Virginia June 2002.

35. Lumley, J.S. "ASR Suppression by Lithium Compounds", *Cement and Concrete Research*, V. 27 (2), 1997, p. 235-244.

36. McCoy, W.J., and Caldwell, A.G. "New Approach to Inhibiting Alkali-Aggregate Expansion," *ACI Journal*, V. 22, No. 9, p. 693-705, 1951.

37. McKeen, R.G., Lenke, L.R., Pallachulla, K.K., and Barringer, W.L. "Mitigation of Alkali-Silica Reactivity in New Mexico", Transportation Research Record 1698, Concrete 2000, Paper No., 00-1216, National Research Council, p.9-16.

38. Mo, X. "Laboratory Study of LiOH in Inhibiting Alkali–silica Reaction at 20 °C: A Contribution**",** *Cement and Concrete Research*, V. 35, March 2005, p.499-504.

39. Mo, X., Xu, Z., and Tang, M. "Effectiveness of Li_2CO_3 in Reducing Alkali-silica Reaction Expansion and its Mechanism", in review.

40. Novinson, T. and Crahan, J. "Lithium Salts as Set Accelerators for Refractory Concretes: Correlation of Chemical Properties with Setting Times", *J. ACI Materials*, V. 85, January, 1988, p. 12.

41. Odler, I, Dorr, H. "Early Hydration of Tricalcium Silicate II the Induction Period", *Cement and Concrete Research*, V. 9, May 1979, p.277-284.

42. Ohama, Y., Demura, K., Kakegawa, M. "Inhibiting Alkali-aggregate Reaction with Chemical Admixtures", *Proceedings of the 8^h International Conference on Alkali-Aggregate Reaction*, (Eds. K. Okada, S. Nishibayashi, and M. Kawamura), Kyoto, Japan, 1989, Elsevier Science Publishing Co. Inc., New York, 1990, p. 253-258.

43. Pei-xing, Fu, Liu Yan, Wang Jun-min. "Alkali Reactivity of Aggregates and AAR-Affected Concrete Structuresin Beijing", *Proceedings of the 12th International Conference on Alkali-Aggregate Reaction in Concrete*, Beijing, p. 1055-1061, 2004.

44. Rangaraju, P. and Olek, J. "Potential for Acceleration of ASR in the Presence of PavementDeicing Chemicals." IPFR Project 01-G-002-03-9. 2005.

45. Sakaguchi, Y., Takamura, M., Kitagawa, A., Hori, T., Tomosawa, F, and Abe, M., "The Inhibiting Effect of Lithium Compounds on Alkali-silica Reaction", *Proceedings of the 8^h International Conference on Alkali-Aggregate Reaction*, (Eds. K. Okada, S. Nishibayashi, and M. Kawamura), Kyoto, Japan, 1989, Elsevier Science Publishing Co. Inc., New York, 1990, p. 229-234.

46. Stade, H. "On the Reaction of C-S-H (di, poly) with Alkali Hydroxides", *Cement and Concrete Research*, V. 19, 1989, p. 802.

47. Stanton, T.E. (1940). "Expansion of Concrete Through Reaction Between Cement and Aggregate." *Proceedings of the American Society of Civil Engineers*, Vol. 66, No. 10, pp. 1781-1811.

48. Stark, D.C., Morgan, B., Okamoto, P., and Diamond, S. “Eliminating or Minimizing Alkali-silica Reactivity”, National Research Council, SHRP-C-343, Washington DC, 1993.

49. Stokes, D.S. “Concrete Durability: ASR and Other Deterioration Mechanisms”, Workshop Handbook, FHWA and ACI, June 2001.

50. Thomas, M., Hooper, R., and D. Stokes. “Use of Lithium-Containing Compounds to Control Expansion in Concrete Due to Alkali-Silica Reaction,” *Proceedings of the 11th International Conference on Alkali-Aggregate Reaction in Concrete*, Centre de Recherche Interuniversitaire sur le Beton (CRIB), Canada, 2000.

51. Thomas, M.D.A., Stokes, D., and Rodgers, T. “The Effect of Lithium-based Admixtures on the Properties of Concrete”, *7th CANMET/ACI International Conference on Superplasticizers and other Chemical Admixtures in Concrete*, SP-217, V.M. Malhotra (Ed.), American Concrete Institute, Farmington Hills, Michigan, September 2003.

52. Tremblay, C., Berube, M. A., Fournier, B., Thomas, M. D. A. (2004). “Performance of Lithium-based Products Against ASR: Effect of Aggregate Type and Reactivity, and Reaction Mechanisms”. *Proceedings of the 7th CANMET/ACI International Conference on Recent Advances in Concrete Technology (suppl. Papers)*, Las Vegas (USA), May 2004, pp. 247-267.

53. Wang, H. and Stokes, D.B. "Compatibility of Lithium-based Admixtures with other Concrete Admixtures," *Proceedings of the 10th International Conference on Alkali-Aggregate Reaction (ICAAR)*, Melbourne, Australia, August 18-23, 1996, p. 884-891.